GOLGI POSITIONING DURING CELL MIGRATION

Andrea Christine Uetrecht

A dissertation submitted to the faculty of the University of North Carolina at Chapel Hill in partial fulfillment of the requirements for the degree of Doctor of Philosophy in the Department of Cell and Developmental Biology

Chapel Hill
2009

Approved by:

Dr. James E. Bear

Dr. Vytas Bankaitis

Dr. Patrick Brenwald

Dr. Bob Goldstein

Dr. Steven Rogers

ABSTRACT

Andrea C. Uetrecht

Golgi positioning during cell migration

(Under the direction of Dr. James E. Bear)

Investigation of crucial aspects of cellular function in live cells frequently requires the loss of expression of a specific protein to gain insight into its function. It is also beneficial to combine this with either the enforced re-expression of a tagged version of the protein of interest to validate the phenotype, or the expression of fluorescently tagged marker proteins to investigate a particular phenomenon. Modifications to a short hairpin RNA-mediated knock-down lenti-viral delivery system described here enable the simultaneous expression of short hairpin RNA and a fluorescently-tagged rescue or marker protein to investigate specific cellular processes. The knock-down phenotype of capping protein ß was rescued by the simultaneous expression of a fluorescently tagged knock-down resistant version. Chromophore-assisted laser inactivation of capping protein ß demonstrated the acute loss of function phenotype and highlighted the necessity of loss of endogenous protein expression for the effects to be observed. Another modification in the lenti-viral vector system was used to demonstrate a role for coronin 1B in modulating the rate of actin retrograde flow. A final modification to the lenti-viral

system enabled the simultaneous expression of two different fluorescent markers. This was used to investigate Golgi and nucleus positioning during migration. In Rat2 cells at the edge of an artificial wound, the Golgi and centrosome were positioned coincident to one another and were polarized to the front of the nucleus relative to the wound edge. Freely migrating cells expressing fluorescent markers of the Golgi and nucleus did not exhibit such polarity. Instead, Golgi positioning remained fairly constant relative to the nucleus independent of the direction of migration. Nucleus and Golgi positioning relative to the direction of migration was also independent of the speed or directional persistence. Lamellipodial dynamics such as the distance, duration or rate of protrusion were not substantially different along the nuclear-Golgi axis relative to other areas of the cell periphery. Together these data suggest that Golgi positioning in freely migrating cells is independent of the events at the periphery of the cell that are involved in migration.

Fortune Cookie:
The shortest distance between two points is no fun

ACKNOWLEDGEMENTS

I would like to thank the many people who have provided me with the love, support and guidance that made this all possible. To the IBMS class of 2004 – I could not have asked for a better group of people to start this journey with. How far we have all come in the past 5 years. To my lab-mates past and present – you have made the lab a supportive, fun and entertaining place to be. Thanks especially to Liang and Tom for… well, just being your selves. To my supervisor, Jim Bear – thanks for the opportunity to work on such an interesting project in your lab. I have learned many valuable lessons along the way. To my committee members: Vytas Bankaitis, Pat Brenwald, Bob Goldstein and Steve Rogers – I have appreciated your scientific input and advice greatly, and even more so your unwavering support. Vyto, I hope I can do you proud. Thanks also to Keith Burridge and Ken Jacobson for advice and support. To all of my friends – thanks for your willingness to be dragged to a 'Canes game or two… To Aaron Bradford – thanks for all the love and support you have given me over the years, I couldn't have done this without you and I will always be thankful for having you in my life. To my best friend Nell – you have been my enabler in so many ways… just keep swimming (rabid is good, rabid is wise). To my sister and parents – there simply are no words to express my love and gratitude. Where would I be without you?

TABLE OF CONTENTS

LIST OF FIGURES

LIST OF ABBREVIATIONS

ADF	Actin Depolymerising Factor
APC	Adenomatous Polyposis Coli
aPKC	Atypical Protein Kinase C
CALI	Chromophore-Assisted Laser Inactivation
Coro	Coronin
CMV	Cytomegalovirus
CP	Capping Protein (CapZ)
DOM	Direction of Migration
EGFP	Enhanced Green Flourescent Protein
ECM	Extracellular Matrix
FA	Focal Adhesion
FAK	Focal Adhesion Kinase
FN	Fibronectin
GEF	Guanine nucleotide exchange factor
GSK3	Glycogen Synthase Kinase 3
GT	ß1,4-Galactosyl Transferase
H2B	Histone H2B
IRES	Internal Ribosomal Entry Sequence
KDR	Knock-Down/Rescue
LN	Laminin

LTR	Long Terminal Repeat
MLC	Myosin Light Chain
MSCV	Murine Stem Cell Virus
MT	Microtubule
MTOC	Microtubule Organizing Center
NGA	Nuclear-Golgi Axis
PAK	p21-acivated kinase
PI3K	Phosphoinositide 3-kinase
PIP_2	Phospatidylinositol (4,5)-bisphosphate
PIP_3	Phosphatidylinositol (3,4,5)-trisphosphate
PKB	Protein Kinase B
PLC	Phospholipase C
PM	Plasma Membrane
PTEN	Phosphatase and tensin homolog
ROCK	Rho-associated kinase
shRNA	Short Hairpin RNA
siRNA	Small Interfering RNA
SSH1L	Slingshot 1L
TGN	Trans-Golgi Network
WASP	Wiscot-Aldrich Syndrome Protein

CHAPTER 1: INTRODUCTION

In multicellular organisms, cell migration is a crucial process for both development and tissue homeostasis and is involved in such diverse processes as neuronal targeting [1] and the immune response [2, 3]. Cell migration also plays critical roles in various pathological conditions ranging from rheumatoid arthritis [4] to cancer metastasis [5], making understanding the events that regulate and affect cell migration of fundamental importance.

The Cell Migration Cycle

The field of cell migration has been intensely studied over many decades. The most common studies of cell migration *in vitro* examine the properties of cells on a two dimensional substrate. In this context, cells display a characteristic cycle of migratory events (reviewed in [6]). Migration is initiated through the protrusion of an actin-rich leading edge, accompanied by the formation of small adhesions at the leading edge. This is followed by the localized disassembly of mature adhesions at the rear of the cell, while myosin-mediated contractility causes retraction. Depending on the cellular context, this cycle can occur as discrete steps or in a continuous, smooth fashion. In either case, the cell migration cycle is an inherently polarized process, with protrusion occurring at the front of the cell, and retraction at the back. One central question in the field of cell migration is how protrusive,

retractive and adhesive areas become localized to specific regions within the cell to cause this ‘polarity’ and coordinate migration.

Polarity and Migration – What is Polarity?

Defining Front – Formation of the Lamellipodium

The front of the cell is generally considered to be the actively protruding area at the edge of the cell known as the leading edge or lamellipodium. The events that govern protrusion have been studied in numerous systems. One of the hallmarks of lamellipodial protrusion is elevated levels of phosphatidylinositol (3,4,5)-trisphosphate (PIP_3). PIP_3 is generated at the plasma membrane (PM) through activation of phosphoinositide 3-kinase (PI3K) and contributes to protrusion through the activation of two signaling molecules: phospholipase C (PLC) and Rac. PLC catalyzes the hydrolysis of phosphatidylinositol (4,5) bisphosphate (PIP_2) at the PM. Loss of PIP_2 through PLC-mediated hyrolysis was shown to cause the release of the actin severing protein, cofilin, leading to actin polymerization [7]. Presumably other actin regulatory proteins could be held inactive at the PM by PIP_2 and could also be released by this mechanism resulting in their localized activation, although this remains to be demonstrated. Like PLC, the small GTPase Rac is activated by elevated PIP_3 levels to promote protrusion. Rac activation is accomplished by its recruitment to the PM as well as the activation of Rac-specific guanine nucleotide exchange factors (Rac-GEFs)

Initiation of protrusion via Rac activity, PI3K activity and PIP_3 levels depend on the cellular context. In *Dictyostelium*, PI3K is activated by cyclic-AMP receptor-1

(CAR1) and heterotrimeric G proteins (reviewed in [8]). In neutrophils stimulated with *N*-formyl-Met-Leu-Phe (fMLP), Rac is activated downstream of G-protein coupled receptors [9] in a PI3K-dependent manner [10]. In mammalian epithelial cells, both Rac and PI3K are activated downstream of the epidermal growth factor (EGF) receptor [11] to initiate leading edge protrusion.

Activated Rac recruits members of the Wiscott Aldrich Syndrome protein (WASP)/WASP and Verprolin-homology protein (WAVE) family, which, in turn, cause the activation of the Arp2/3 complex (reviewed in [12]). Arp2/3 promotes actin polymerization through the nucleation of new filaments at a 70° angle to an existing filament to generate a branched dendritic actin network [13]. It is this dendritic actin polymerization that provides the force required for membrane protrusion [14], and also causes the rearward movement of the existing actin meshwork in a process called retrograde flow. A number of other factors also influence actin architecture and thus lamellipodial protrusion. For example, capping protein (CapZ or CP) caps the growing end of filaments, preventing linear growth thereby indirectly promoting branching [15, 16]. Processive cappers such as mDia have the opposite effect, promoting linear actin elongation at the expense of branching (reviewed in [17]). Still other proteins such as the Coronin 1B (Coro1B) isoform affect actin architecture through influencing localized turnover and disassembly [16, 18].

Together the factors discussed above contribute to the formation and protrusion of the leading edge. However, using the leading edge as a marker of 'front' is problematic due to the frequent occurrence of multiple protrusive regions in many contexts.

Defining Rear – Contraction and Retraction

Recent evidence suggests that the rear or trailing edge of the cell is defined prior to the establishment of front. For example, Mseka and colleagues have shown that in embryonic chick fibroblasts, the first visible break in cell symmetry following the washout of the actin destabilizing drug Latrunculin A is a localized area of retraction. Prior to retraction or migration, bundled actin filaments become aligned along the direction of migration. The symmetry-breaking event occurs at one end of the bundled actin and requires the activity of the actin depolymerizing factor (ADF)/cofilin family of actin severing proteins. When protrusion and migration are initiated approximately 20 minutes after washout the area of retraction becomes the rear of the cell [19].

The formation and stabilization of actin bundles, as well as the formation of a well-defined, extended cell rear requires activated myosin light chain (MLC) in cooperation with myosin II isoforms [20]. Myosin activity and actin contractility are regulated by the small GTPase RhoA and its downstream effector Rho-associated kinase (ROCK). These are localized to the sides and rear of migrating cells in both *Dictyostelium* [21] and neutrophils [22] where they limit protrusive activity. In *Dictyostelium*, localization and activity of phosphatase and tensin-homolog (PTEN) is required for localized RhoA and myosin activity [21]. Rho-mediated actin contractility defines the cell rear and limits protrusive activity away from the front.

Establishing vs Maintaining Polarity – the Rho GTPases

Productive translocation of the cell requires that the spatial organization of protrusion, retraction, and adhesion be maintained over a period of time. Clearly,

cells have some self-organizing capacity that allows protrusion to be coupled with adhesion, and retraction with de-adhesion, as well as locally reinforcing these activities through feedback loops. Each of the small GTPases of the Rho family play important, yet distinct, roles in this process. As discussed above, PI3K-mediated PIP_3 production causes the activation of Rac [9]. Rac, in turn, has been found to activate PI3K [23-25] leading to increased PIP_3 production, and thus to enhanced actin polymerization and protrusion [26]. Actin polymerization, in turn, also amplifies PIP_3 levels at the front [24]. This creates a positive feedback loop for the establishment and maintenance of leading edge protrusion.

PI3K may also be involved in inhibiting the signaling networks that define the back of the cell. Activity of the PI3K isoform p110δ in macrophages negatively regulates PTEN through the inhibition of RhoA/ROCK [27], and thus may serve to inhibit “back-ness”, while reinforcing “front-ness”.

Similarly, at the sides and rear of the cell, protrusive activity is restricted by Rho-mediated contractility. In stimulated neutrophils, RhoA/ROCK activity is required for the activation and recruitment of PTEN to the posterior membrane [28]. Loss of PTEN in *Dictyostelium* results in defective recruitment of myosin II and the failure to suppress lateral pseudopods [21]. As well, the PIP_3-phosphatase activity of PTEN serves to further antagonize “front” signaling through the localized depletion of PIP_3. RhoA, ROCK and PTEN thus form a feedback loop, and together are responsible for maintaining the cell rear.

The roles of Cdc42 are less clear. The spatial restriction and maintenance of persistent leading edge protrusion has been shown to be dependent on Cdc42

activity in neutrophils [26] and astrocytes [29], yet in fibroblasts reduced Cdc42 expression has no effect on either the speed of migration or directional persistence [30]. Instead, reduced Rac expression and activity results in decreased peripheral lamellae and increased directional persistence in fibroblasts [30]. It is not clear whether these represent cell-type differences in the roles of Rac and Cdc42, or whether they reflect context-dependent differences in the steady-state activities or localization of other factors. For example, plating conditions could affect basal RhoA activity, which would affect the activities of other factors through the feedback loops described above. An additional role for Cdc42 in establishing or maintaining the organization of internal structures is discussed later in this chapter; how this Cdc42-mediated internal polarity might contribute to protrusion or migration remains to be demonstrated.

The Role of Adhesions

The localized formation, maturation and turnover of adhesions are important for migration. Adhesions serve as a direct link between the cell and the substratum, and the traction they provide is an absolute requirement for productive lamellipodial protrusion. On the other hand, strong adhesions can be an impediment to migration, by hindering retraction at the cell rear.

The adhesive interaction between the cell and the extracellular matrix (ECM) is mediated by integrins, a large family of single-pass heterodimeric transmembrane proteins that bind specifically to ECM proteins such as fibronectin (FN), laminin (LN) and collagen. The intracellular domain links integrins to the actin cytoskeleton through large protein complexes that can contain in excess of 150 different proteins,

including talin, paxillin, vinculin, α-actinin, integrin-linked kinase, focal adhesion kinase (FAK) and Src, among many others (reviewed in [31-33]). The precise composition varies considerably depending on the cell type, the integrins involved, and a number of other interrelated factors, including the sub-cellular location, size, maturity, and tension of the adhesion. Integrin activation is mediated by PIP_2 and talin [34]. Talin produces conformational changes in integrins, possibly through separation of the transmembrane helices, causing activation and allowing them to engage ECM ligands ([35], reviewed in [36]). Talin also directly binds the actin cytoskeleton [37], thus integrin-ECM engagement links the actin cytoskeleton to the extracellular environment.

In migrating cells, integrin engagement with ECM is initiated in association with the leading edge, often at the base of filopodia or actin ridges. These nascent adhesions or focal complexes are characterized by their small size and short life, and are associated with parallel bundles of actin (reviewed in [38]). Focal complex formation depends on fast actin retrograde flow from the lamellipodium, with complexes forming at the transition zone between the lamellipodial and lamellar regions [39, 40]. The force generated by retrograde flow is thought to lead to the recruitment of other proteins, presumably through tension-sensing activation. However, the precise mechanisms responsible for the recruitment or activation of each component, and the effects of each component on adhesion formation, stability and disassembly are still being elucidated. Here we focus instead on general spatiotemporal aspects of adhesion dynamics.

In the absence of additional force, focal complexes fail to mature and are rapidly disassembled. However, Rho-mediated contractility or the external application of force on the associated actin fibers causes focal complexes to transition into focal adhesions (FA) [41]. This initiates a feedback loop in which actin-mediated tension on the adhesion causes the recruitment of additional proteins, causing a growth in adhesion size, an increase in the number of associated stress fibers, and thus an increase in actin-mediated tension on the adhesion. Mature focal adhesions are therefore characterized by their larger size and longer lifetime as well as with the presence of additional proteins and the association with actin stress fibers, or antiparallel bundles of contractile actin (reviewed in [38, 40]). Mature adhesions are located under the cell body and at the periphery, but are specifically absent from the lamellipodium.

Just as the formation of focal complexes is essential for leading edge protrusion at the front during cell migration, the turnover and disassembly of focal adhesions at the rear of the cell is necessary for cell retraction. Microtubules (MTs) are known to target focal adhesions throughout the cell, and these targeting events are correlated with either decreased growth or disassembly of focal adhesions [42]. Indeed, the MT targeting frequency at the retracting edge of the cell is several-fold higher than at the protruding edge [42], highlighting the importance of these events. MT targeting could facilitate adhesion turnover through the delivery or removal of multiple signaling proteins or complexes, but the precise cargo is not yet known. Possibilities include complexes involved in relieving tension, for example Rho inhibitors or Rac activators. Candidates for this are the Rho/Rac-GEFs Lfc [43] and

GEF-H1 [44], the Rac-specific GEF Asef [45] or p21-activated kinase (PAK; [46]). Delivered locally, these factors could cause relaxation of the associated stress fiber, allowing for disassembly of the focal adhesion [47]. Additionally, proteolytic enzymes that mediate cleavage of adhesive proteins could also facilitate FA disassembly. The protease calpain is required for MT-mediated FA turnover following nocodazole washout [48]. Calpain-mediated cleavage of talin [49] and/or other FA components could cause a conformational change in integrins leading to either α-actinin binding [48, 50] or perhaps even disengagement from the ECM. However FA turnover is mediated, it is clear that the spatiotemporal regulation of focal adhesion formation, maturation and disassembly is crucial for efficient cell migration.

Directed Migration

Here we define directed cell migration as the orientation of migration along a specific axis based on external cues. Many different factors can effect directed cell migration. For example, at the edge of an experimental wound the geometric constraints and cell signaling molecules provided by neighboring cells causes cells to migrate in a directed manner to fill in the wound [51]. Likewise, a gradient of soluble factors can cause a type of directed cell migration called chemotaxis [52, 53]. Other types of directed migration also occur, but are beyond the scope of this introduction. These include electrotaxis (migration along an electric current) [54], durotaxis (migration along a gradient of matrix stiffness) [55], and haptotaxis (migration along a gradient of deposited ECM) [56].

Migration in to an Experimental Wound

Some of the earliest studies to examine directed cell migration made use of the scratch-wound or wound healing assay. In this assay, a confluent monolayer of cells is experimentally 'scratched' to remove a strip of cells. The remaining cells at the edge of the experimental wound subsequently polarize and migrate into the cell-free zone, thereby closing the wound. Early observations indicated that external polarization and migration into the wound was also accompanied by polarization of internal structures such as the microtubule organizing center (MTOC)/centrosome, Golgi apparatus, and nucleus. The first study to look at MTOC positioning in this context found that in pig thoracic aorta endothelial cells 4 to 44 hours after wounding, the MTOC was oriented between the nucleus and the wound edge in 80% of cells at the edge of the wound and in 70% of cells in the 2nd and 3rd rows back from the wound edge [51]. Similarly, in NRK fibroblasts 78% of cells at the wound edge had both the Golgi and MTOC positioned between the nucleus and the wound edge within 5 hours of wounding [57]. Indeed, by 5 minutes, before visible lamellar extension into the wound, 60% of cells displayed Golgi and MTOC polarity. Based on this, the authors speculated that MTOC and Golgi positioning might play several important roles in specifying the direction of migration (DOM). It was suggested that polarization of the MTOC was responsible for positioning the force-generating system involved in lamellipodial protrusion (that actin provided the force was not known at the time) and for delivering Golgi-derived vesicles. The positioning of the Golgi was speculated to facilitate protrusion through the insertion of new membrane at the leading edge, as well as being involved in the directed secretion of ECM molecules for the formation of new adhesions. Another study

showed two stages of reorientation exhibited by NIH 3T3 fibroblasts [58]. In the initial stage (up to 3 hours post wounding) cells become polarized, with the nucleus and stress fibers at the rear of the cell and endosomes and mitochondria facing the direction of migration but excluded from the lamellipodium. In the second stage of migration, stress fibers disappear from the cell rear, while the mitochondria and endosomal compartments can be seen in the lamellipodia, even sometimes approaching the leading edge. Whether these stages occur in other cell types is unclear, and it is becoming increasingly evident that the mechanisms responsible for polarization and migration into an experimental wound differ significantly from one cell type to another. Perhaps the most striking example of this is that PtK2 cells [59] and MCF10a cells [60] polarize with either the centrosome or the MTOC and Golgi, respectively, to the rear of the nucleus. However, other more subtle differences between cell types are also being discovered.

Mechanisms of Positioning – Actin and Microtubule Dependence

The mechanism(s) responsible for Golgi, MTOC, and centrosome positioning are being elucidated, and may depend upon actin, microtubules, or both, depending on the cell type. In many cell types, the cell centroid roughly coincides with the position of the centrosome or MTOC [61], around which the Golgi is organized (reviewed in [62]). In BSC-1 cells the centrosome is positioned either coincident with, or within 5μm of, the cell centroid in 89% of wound edge cells [61]. As leading edge extension proceeds and the cell centroid shifts forward, the centrosome is maintained at a central position in a MT-dependent manner, while nuclear movement is delayed, initially remaining stationary, and subsequently lagging behind

the centrosome [61]. Centrosome repositioning under these conditions is thus a result of the MT-dependent forward movement of the centrosome, due to leading edge protrusion rather than rearward nuclear movement. Other studies in NIH 3T3 cells, however, demonstrate that the nucleus is repositioned behind the MTOC following wounding through rearward movement of the nucleus in an actin- and myosin-dependent manner even in the absence of protrusion [63]. In pig thoracic aorta endothelial cells inhibition of MT dynamics through treatment with Colcemid blocks both MTOC reorientation and migration into the wound, while treatment with Cytochalasin B to block actin dynamics delays MTOC reorientation in the first row of cells, prevents reorientation in the 2nd and 3rd rows, and blocks migration completely [64]. In astrocytes, both MTOC polarity and migration into the wound are actin dependent, as treatment with Cytochalasin D blocks both behaviors, but surprisingly does not block protrusion formation. Treatment with Taxol or low levels of Nocodazole to block MT dynamics blocks both protrusion formation and MTOC orientation [29] suggesting that both protrusion and MTOC polarity are MT-dependent events in astrocytes.

Signaling Networks Involved in Wound-Edge Polarity

The differences in MT and actin dependence observed from one cell type to another suggests that not only do the mechanisms involved in positioning vary between cell types, but also that the signaling networks involved might differ as well. In both NIH 3T3 fibroblasts [63] and astrocytes [29], polarization of the MTOC relative to the nucleus occurs downstream of the Cdc42/Par6/aPKC polarity complex, and also requires dynein activity. In astrocytes, Cdc42/Par6/aPKC and

dynein are required, in addition to GSK-3 and APC [65], for proper MTOC polarity, but not for the formation of protrusions. However, they are required to restrict protrusion formation to the wound edge. In contrast, rat embryonic fibroblasts do not require Par6/aPKC to restrict protrusive activity to the wound edge, but require the activity of PAK, downstream of Cdc42 [66]. In NIH 3T3 fibroblasts, Cdc42/Par6/aPKC and dynein are required for self-centering of the MTOC, and thus polarity [63]. Together these studies demonstrate that the wound edge represents a situation in which similar signaling networks simultaneously govern both directional migration and internal organization of the cell.

Chemotaxis

Chemotaxing cells are characterized as being highly polarized, with a well-defined lamellipodial region extending towards the chemotactic source and a retracting tail. Classic models for chemotaxis rely on the internal amplification of a shallow external chemotactic gradient. This occurs through the local activation and amplification of PIP_3 signaling where receptor occupancy is highest coupled with the global inhibition of PIP_3 signaling, via PTEN, throughout the remainder of the cell. This feedback loop is proposed to render the front of the cell more sensitive to the chemoattractant and lead to directionally persistent migration towards the source. Recent studies, however, suggest that this model may not be entirely complete. *Dictyostelium* cells lacking both PTEN and all five PI3K isoforms exhibit slower migratory speeds but are not defective in directional sensing [67]. Similarly, neutrophils lacking PI3K are less migratory but still respond to chemotactic gradients [68]. Additionally, cells in very shallow gradients undergo chemotaxis through a

characteristically different type of migratory path called a biased random walk. In this case, migration is the result of a series of discrete protrusion events that are either formed preferentially towards the chemotactic source, as demonstrated for dendritic cells and fibroblasts [69], or are preferentially maintained towards the source as demonstrated in *Dictyostelium* [70]. In the latter context, the inhibition of PI3K affects the frequency of protrusive events, but not their accuracy [70]. During biased random walk chemotaxis, protrusions can occur in any direction at any given time, but the net protrusive activity, and thus the net DOM, is towards the chemotactic source.

Few studies have examined centrosome or Golgi positioning during chemotaxis. In chemotaxing neutrophils the centrosome is positioned preferentially between the lamillipod and the nucleus [71]. Similarly, mouse peritoneal macrophages reorient both the Golgi and MTOC towards a gradient of activated mouse serum in an actin-dependent manner [72]. In chemotaxing *Dictyostelium*, the centrosome is positioned to the front of the nucleus, and if the position of the gradient is altered, centrosome repositioning follows the formation of a new leading process [73].

Unconstrained Migration

Observations of MTOC and Golgi polarity and migration suggest that there is a fundamental link between MTOC/Golgi polarity and migration. Few studies have attempted to address this problem directly in freely migrating cells in the absence of external cues. Danowski et al. reported that the centrosome of freely migrating PtK2 cells expressing green fluorescent protein (GFP)-tagged γ-tubulin did not reorient

when the cell changed direction, and in fixed cells was localized predominantly to the rear of the nucleus, often in the retracting tail [74]. In the context of the wound edge the positioning of the centrosome in this cell type was maintained the rear of nucleus [59], demonstrating that anterior positioning of the MTOC relative to the nucleus is not a requirement for migration. Ueda et al. examined centrosome positioning in *Dictyostelium* using GFP-γ-tubulin expression and found that centrosome repositioning never precedes pseudopod extension. However, if reorientation of the centrosome does not occur within 30 seconds the new pseudopod will collapse [73], suggesting that centrosome positioning is important for the stabilization or maintenance of the leading process.

The positioning of the Golgi has never been examined in freely migrating cells. However, the observed co-localization of the MTOC and Golgi in other contexts would suggest that, like the centrosome, Golgi positioning might be important for cell migration, leading to several important questions.

- **Does the Golgi Polarize in the Absence of External Cues?**

  Golgi positioning could be correlated with the DOM or migratory path of freely migrating cells. Based on available data on MTOC/centrosome and Golgi positioning in the situations discussed above, it seems reasonable to speculate that Golgi positioning would correlate with the DOM, at least during periods of highly persistent migration.

- **Does Golgi positioning influence lamellipodial dynamics?**

  One of the purposes ascribed to Golgi positioning is to facilitate targeted delivery of post-Golgi vesicles to the leading edge of the cell. Presumably this would result in the localized delivery of either signaling complexes or bulk membrane

that would be required for protrusion. If this is the case, lamellipodial dynamics could be affected by proximity to the Golgi. It is also possible that all lamellipodia are targeted equally, and/or that localized vesicle fusion has no effect on lamellipodial dynamics.

- **What signaling pathways couple Golgi positioning to migratory parameters?**

  Assuming that Golgi positioning is correlated with either differences in lamellipodial dynamics or the DOM (or both), are any of the signaling pathways implicated in polarity in other contexts relevant for freely migrating cells? Loss of a particular signaling pathway could result in a number of different phenotypes. Uniform lamellipodial dynamics could indicate defects in vesicle targeting to the front. Changes in cell speed, or persistence, or loss of Golgi polarity, could indicate roles in coupling Golgi positioning to the DOM. Alternatively, loss of a particular signaling pathway could have no effect on lamellipodial dynamics, migration, or Golgi polarity.

In order to examine these questions, we developed and tested a series of expression constructs to simultaneously knock-down target genes while expressing, at modest levels, either a fluorescently tagged rescue protein, or fluorescent marker(s). The design and testing of the initial constructs are outlined in Chapter 2. Our success with these constructs prompted us to build a 'polarity sensor' that fluorescently tags both the nucleus and Golgi from the same vector backbone (outlined in Chapter 3). This allowed us to pursue whether Golgi positioning was correlated with the DOM or other migratory parameters (outlined in Chapter 3), or with differences in lamellipodial dynamics (outlined in Chapter 4). We find that Golgi positioning is not related to either lamellipodial dynamics or migratory parameters, precluding investigation of any signaling pathways involved.

CHAPTER 2: DEVELOPMENT OF KNOCK-DOWN/RESCUE SYSTEM

Summary

RNA interference has become a common cell biology technique. Here we describe modifications to a lentiviral-mediated short hairpin RNA delivery system for a broad spectrum of applications. We demonstrate its use in replacing endogenous protein with a fluorescently tagged version to rescue knock-down phenotypes. We also demonstrate its use to mark short hairpin RNA targeted cells with fluorescently labeled proteins to examine protein dynamics in live cells containing either shRNA against the protein of interest or a non-specific control short hairpin RNA. Finally, we describe a modification allowing for the simultaneous expression of two proteins from the same promoter. Based on our success in these initial studies, we continue to use this system for knock-down of target proteins and are expanding upon both the short hairpin RNA targets as well as the range of fluorescent markers for use in future studies.

Introduction

The technique of RNA-mediated interference (RNAi) of protein expression has become increasingly prevalent in cell biology. There are several common approaches to target specific proteins for knock-down. The first technique is to transfect either a single species or a cocktail of double stranded small interfering

RNA (siRNA) that is complimentary to sequence(s) in the target protein. There are several drawbacks to this technique. It is often difficult to unambiguously identify which cells received the siRNA even when simultaneously co-transfected with a fluorescent marker. Additionally, because the siRNA is delivered by transfection, researchers are limited to using easily-transfected cell types. Finally large amounts of siRNA may cause off-target effects such as increased expression of the cellular RNAi processing machinery.

Another commonly used technique for inducing RNAi involves the generation of an expression vector encoding a specific sequence that will become processed into short hairpin RNA (shRNA). This approach can overcome some of the disadvantages of the siRNA approach described above. First, the vector can be engineered to also express a GFP marker, allowing for unambiguous identification of targeted cells. Second, a vector-based system is self-renewing. Finally, if the shRNA system is incorporated into a viral vector delivery system, the range of target cells is much greater as viral delivery is independent of transfection efficiency and the sequence becomes stably integrated into the genome of the targeted cells. However, as with siRNA-mediated knock-down, vector-based shRNA delivery systems cannot overcome the possibility of off-target effects. In either case, the knock-down phenotype must be validated by rescuing the phenotype through the re-expression of the target protein.

Rubinson et al. reported the use of a lentiviral-mediated shRNA delivery system to infect a broad range of cells [75]. We initially set out to create a single-step knock-down/rescue system based on this vector. Our success with this

prompted further modifications to substantially increase the utility of the system. These changes and a sample of their applications are discussed in this and the following chapter.

Results and Discussion

In creating our knock-down/rescue system, we wanted to minimize the possibility of inducing additional phenotypes as a result of the overexpression of the rescue construct. We therefore wanted to ensure that target protein re-expression levels were close to physiological. We tested GFP expression levels from several different promoters and found that the expression from the 5' long terminal repeat (LTR) from the murine stem cell virus (MSCV) was considerably lower than from the cytomegalovirus (CMV) promoter used in the original pLL3.7 vector (not shown).

Validation of Knock-Down/Rescue

We set out to test for the ability of the 5'LTR promoter to rescue protein expression to near-endogenous levels, as well as to rescue a knock-down phenotype. We used a previously characterized shRNA against the ß-subunit of the actin capping protein, CapZ (CP), which is effective against mouse and rat CP [16], but has two mismatches with human CP (Figure 1A). We then generated a series of constructs incorporating either or both of the CP-shRNA (shCP) and/or MSCV-5'LTR-driven human EGFP-CPß (Figure 2). From these vectors we generated stable cell lines in Rat2 fibroblasts. As previously reported, expression of the shCP resulted in the formation of increased numbers of filopodia [16], while the co-expression of EGFP-CP was able to rescue the phenotype (Figure 1B). A stable

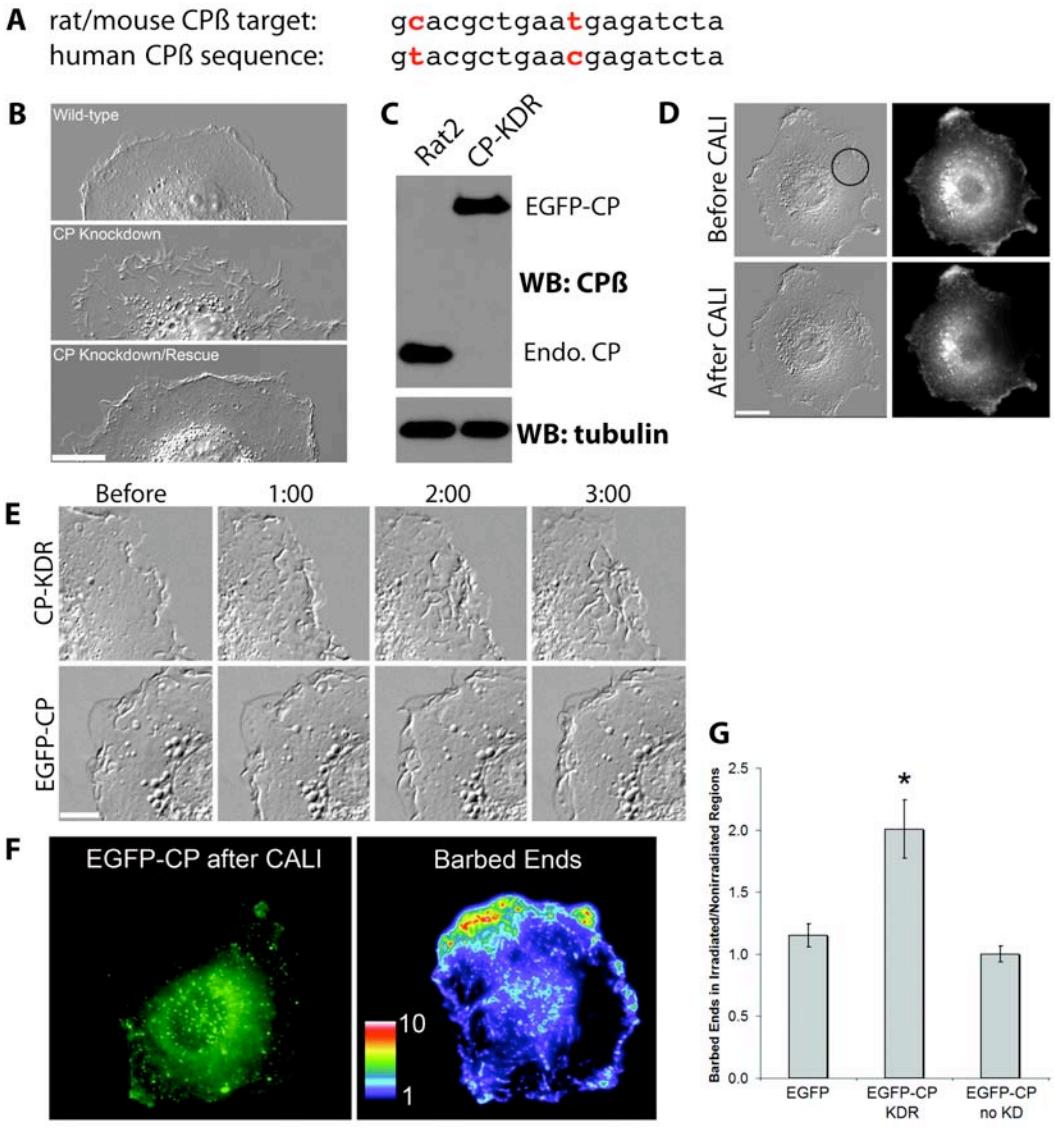

Figure 1: CPß knock-down/rescue and CALI of EGFP-CP.

A) Alignment between rat/mouse shRNA target sequence and the corresponding human sequence with two mismatches indicated in red.

B) DIC images of an uninfected control Rat2 fibroblast (top) and Rat2 cells infected with only the shCP portion of the vector (middle) or the complete KDR construct (bottom).

C) Western blot of control Rat2 cells and a clonally derived Rat2 cell line infected with the KDR construct. Alpha-tubulin is used as a loading control (bottom panel).

D) DIC images of a Rat2 CP-KDR cell before and 3 min after CALI (left) and fluorescent images of the same cell before and immediately after CALI (right). Black circle indicates the area of irradiation.

E) Time-lapse DIC images of the irradiated region of a CP-KDR cell (top) or a cell expressing EGFP-CP without knock-down of endogenous protein (bottom).

F) Fluorescent image of EGFP-CP immediately after laser irradiation (left) and a pseudocolored image of actin filament barbed ends 3 min post-CALI.

G) Graph showing the relative barbed end increase in the irradiated regions of Rat2 cells expressing EGFP alone (n=12), CP-KDR (n=19), or EGFP-CP with no knock-down of endogenous CP (n=7)

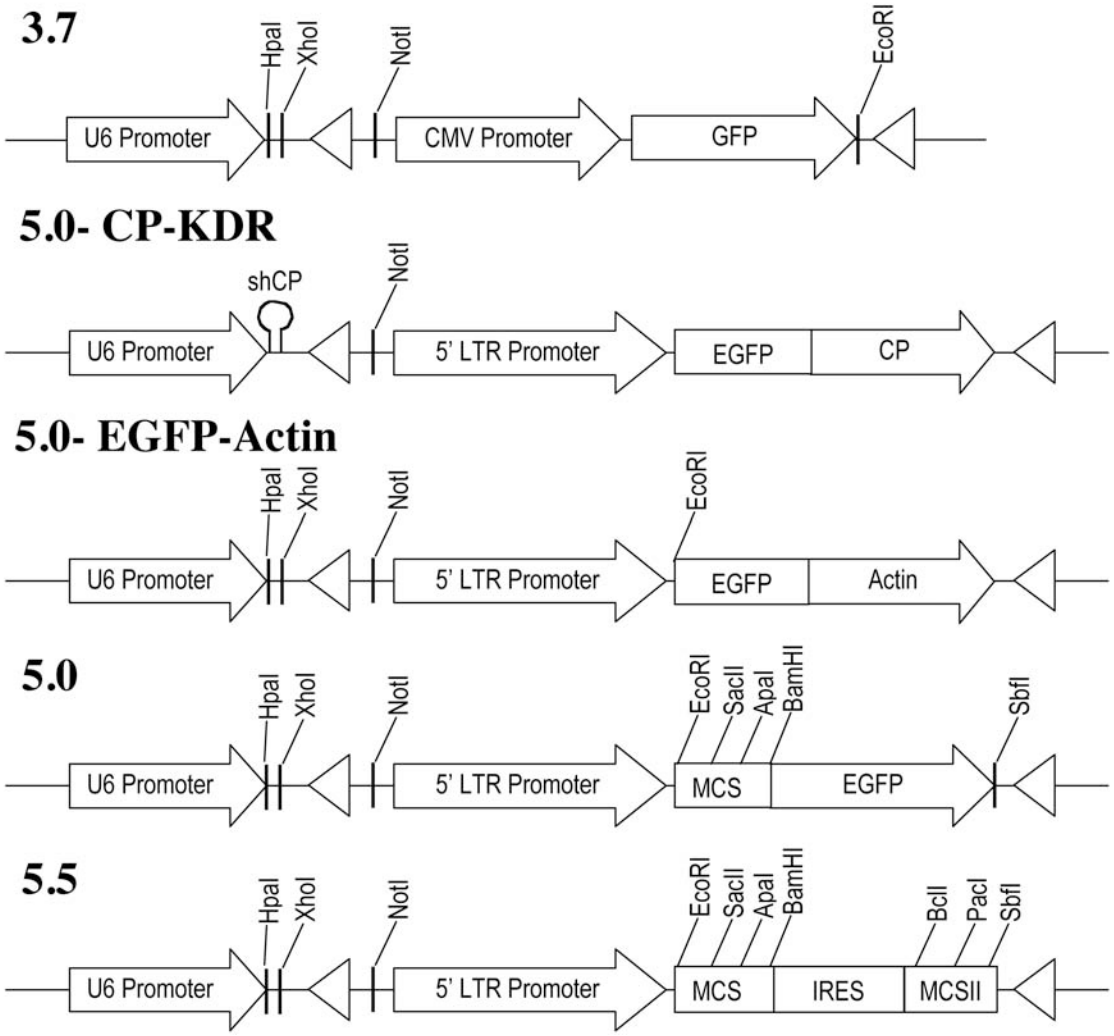

Figure 2: Schematic of lenti-lox vector design.

The original lenti-lox vector, pLL3.7 is shown at the top. Modifications to this vector included the generation of the 5.0 series of lenti-lox vectors where expression of the fluorescent rescue or marker protein is under control of the MSCV 5'LTR promoter. In pLL 5.5 the EGFP was replaced with an internal ribosomal entry sequence (IRES) to allow simultaneous expression of multiple proteins from the same promoter.

clonal cell line generated from this knock-down/rescue (KDR) construct displays complete loss of endogenous CPß, while expressing near-physiological levels of the EGFP-tagged human CPß as detected by Western blot analysis (Figure 1C). It is important to note that the antibody used to detect protein levels recognizes a region of CPß that is identical between human and rat; therefore similar band intensities reflect similar protein expression levels. Because the expression levels of MSCV-5'LTR-driven EGFP-CPß so closely matched endogenous CPß protein levels, we based all further expression constructs on the MSCV-5'LTR promoter.

Based on our success with this construct, we also constructed a similar vector to facilitate use in other applications. Specifically, a multi-cloning site was cloned upstream of EGFP, under the control of the MSCV-5'LTR promoter (pLL5.0, Figure 2). We used this approach to confirm the knock-down phenotype of Coro1B, again targeting rat/murine Coro1B specifically and rescuing with EGFP-tagged human Coro1B (hCoro1B-EGFP) which has four mismatches in the shRNA target sequence (Figure 3A). Expression of shCoro1B alone results in a slower migratory speed, as well as a decrease in lamellipodial protrusion distance and duration (Figure 3B-D). These effects are rescued by the expression of hCoro1B-EGFP, indicating the functional replacement of rat Coro1B with GFP-tagged human Coro1B.

This knock-down/rescue system has also been used to confirm the knock-down phenotype of Coro2A [76] and is currently being used for other applications. To expand the versatility of this system, we have also replaced the EGFP tag with red fluorescent proteins (mCherry or TagRFP), and have generated a bi-cistronic vector with an internal ribosomal entry sequence (IRES) flanked by two

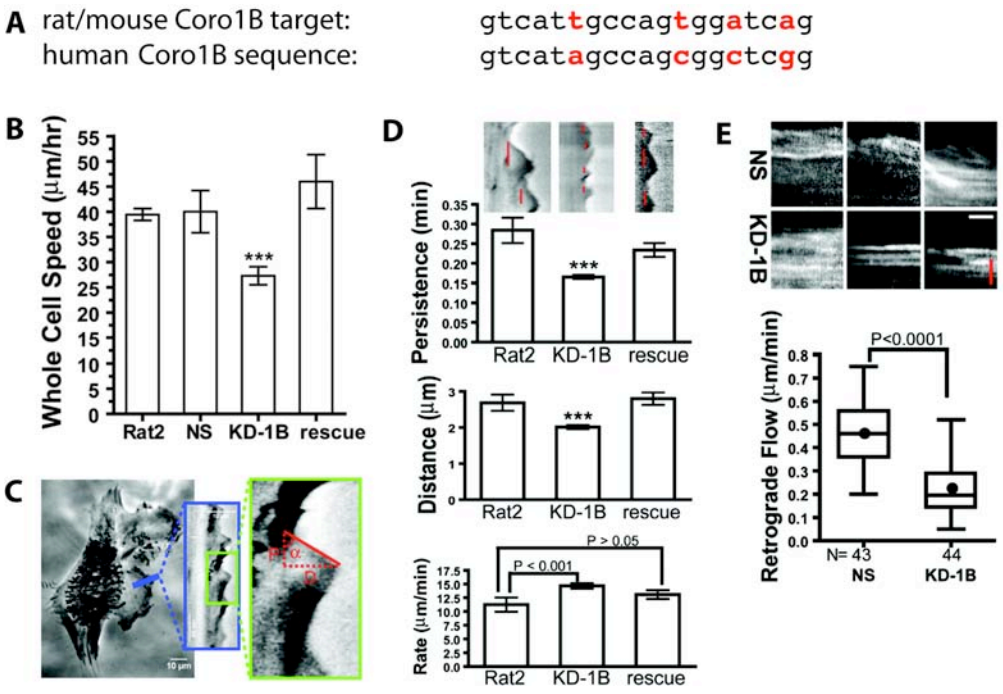

Figure 3: Coro1B knock-down/rescue and knock-down/marker.

A) Alignment between rat/mouse shRNA target sequence and the corresponding human sequence with four mismatches indicated in red.

B) Whole cell speed of uninfected Rat2 control cells or Rat2 cells expressing a non-specific hairpin (shNS), the Coro1B target (KD-1B) or the Coro1B-KDR (rescue). Newman-Keuls multiple comparison test was used after one-way ANOVA to generate the p values ($p < 0.001$); error bars represent 95% CI.

C) Method for kymography analysis. Minimal intensity projection of a 300-frame 1 s interval movie is presented on the right. Pixel intensities along a 1-pixel wide line (blue) were used to generate the kymograph presented in the blue box; a magnified region (outlined in green) is displayed on the right. Red dashed lines indicate the parameters for one protrusion. Abbreviations are as follows: D, protrusion distance; P, protrusion persistence; and tanα, protrusion rate.

D) Protrusion parameters of Rat2 cells expressing the Coronin 1B shRNA without or with coexpression of human Coronin 1B (rescue). Sample kymographs are shown above each bar; red lines indicate persistence time for each protrusion. Mean value is presented; error bars represent 95% CI. Newman-Keuls multiple comparison test was used after one-way ANOVA to generate the p values ($p <$

0.001 compared to Rat2).

E) Average actin retrograde flow rates in Rat2 cells coexpressing either Coronin 1B (KD-1B) or control (NS) shRNA and GFP-actin. Representative kymographs showing retrograde actin flow are shown above (red bar represents 1.14 mm; white bar represents 30 s). Box and whisker plots represent three measurements/cell for each condition. Unpaired Student's t test indicates a signification difference between samples ($p < 0.0001$).

multi-cloning sites to allow simultaneous expression of two proteins (pLL5.5, Figure 2, discussed below and in Chapter 3).

Other Applications for the Knock-Down/Rescue System

Long-term loss of protein expression, via genetic loss or RNAi, can result in unknown and unanticipated compensations at the cellular level. We have used the CP-KDR cells described above to acutely inactivate CP by using chromophore-assisted laser inactivation (CALI). In this case, EGFP serves as the chromophore and has the advantage of being genetically encoded and thus specifically and covalently linked to the target protein. This eliminates the potential for non-specific labeling that other strategies suffer from [77, 78]. Following CALI of a ~23μm diameter area (approximately 1/6-1/4 of the cell area) using a 1.5mW/μm^2 illumination for 100ms, we observed numerous dynamic protrusions on the dorsal surface of the irradiated area (Figure 1D). This effect was not observed in either cells irradiated over a smaller area at a higher intensity (~5μm, 6.1mW/μm^2; not shown), or in cells retaining endogenous unlabeled protein (lacking the shCP component; Figure 1E). The rapid turnover of CP that we observed with fluorescence recovery after photobleaching (FRAP; not shown) can account for these effects. The rapid turnover and diffusion of non-inactivated EGFP-CP from outside the irradiated area could readily compensate for any acute loss of labeled and inactivated CP, as could the presence of endogenous unlabeled CP. That the CALI effects were not observed in cells retaining endogenous CP also demonstrates that the increase in dorsal surface protrusions is a direct and specific result of loss of CP function rather than a non-specific effect of laser irradiation. We also confirmed

that these dorsal structures contained increased amounts of F-actin as visualized by phalloidin staining (not shown). The barbed end assay indicated the irradiated area contained twice as many barbed ends as the surrounding area of the cell (Figure 1F), consistent with the localized uncapping of actin filaments following CALI. Importantly, no increase in barbed ends was observed in the presence of endogenous unlabeled CP (Figure 1G).

In the above study, we demonstrated not only the utility of EGFP as a CALI fluorophore, but also the necessity of eliminating endogenous protein for the CALI effect to be observed. Another context in which endogenous protein might interfere with the testing of (or compensate for) the tagged construct is during the characterization of mutant proteins. Our knock-down/rescue system can also be used for this application. For example, Coro1B contains a coiled-coil region that mediates homo-oligomerization. Thus, the potential for endogenous protein to interact with and compensate for a mutant Coro1B could confound interpretation of the results. To exclude this possibility, our KDR system was used to identify the actin-binding site on Coro1B as Arg30 and to characterize the role of actin binding in Coro1B function [79]. Specifically actin binding was found to be essential for Coro1B lamellipodial localization and is required to rescue defects in migration and lamellipodial dynamics exhibited by Coro1B knock-down [79].

Marking Knock-down Cells with Other Fluorescent Proteins

Having validated a knock-down phenotype, it is often useful to investigate specific cellular processes using fluorescently tagged proteins. The lentiviral vector system described above can also be used to mark knock-down cells with a particular

protein of interest, simply by cloning the gene of interest into the MCS or replacing the EGFP with another fluorescently tagged protein. As an initial test of this system, we replaced the EGFP with EGFP-actin (Figure 2), followed by cloning of different shRNA sequences including a non-specific sequence (shNS) that has no complimentary sequence in the mouse, rat or human genomes. This allowed us not only to identify infected cells by the expression of EGFP-actin, but also to examine and compare actin dynamics in live cells. Using this approach, we determined that cells expressing shCoro1B knock-down display decreased actin retrograde flow relative to the shNS control cells (Figure 3E). We also used this system to examine the localization of slingshot 1L (SSH1L)-GFP in shCoro1B and shNS cells and found SSH1L localization to be perturbed in Coro1B knock-down cells compared to the shNS control cells (not shown). This system has also been used to examine focal adhesion dynamics using GFP-paxillin in Coro2A knock-down cells [76] and other studies are ongoing.

As demonstrated above, the design of this vector system allows for its use in a broad range of applications. Further modifications of the vector have enabled the simultaneous expression of multiple fluorescent markers from the same promoter by using an internal ribosomal entry sequence (IRES) to create a bi-cistronic vector (pLL5.5, Figure 2). This co-expression system could also be used in cases where the rescue protein does not tolerate the presence of a large tag such as GFP by simultaneous expression of an untagged version of the protein of interest and GFP. This would allow infected cells to be marked by GFP expression without interfering with the function of the protein of interest. Further studies utilizing these knock-

down/rescue and knock-down/marker systems are ongoing. An application for the bi-cistronic expression construct is described in the following chapter.

Materials and Methods

Materials

Cells were from ATCC, restriction enzymes were from New England Biolabs, KOD DNA polymerase was from EMDbioscience. All other materials were from Sigma unless otherwise indicated.

Molecular Cloning

The original lenti-lox vector, pLL3.7 is described in [75]. CPß was cloned from human first-strand cDNA using standard PCR techniques and cloned into pMSCV-EGFP. To generate all pLL3.7-based vector derivatives, the ApaI and SacII sites in the pLL3.7 backbone were sequentially eliminated by enzyme digest followed by Klenow-mediated overhang fill-in and re-ligation. Similar strategies were employed to generate pLL5.0 and pLL5.0-EGFP-CPß. The MCS + EGFP for pLL5.0 or EGFP-CPß for pLL5.0-EGFP-CPß were amplified from pML^2-EGFP or pMSCV-EGFP-CPß, respectively, using standard techniques. The 5'LTR from pMSCV was amplified using primers that overlapped with either the MCS or EGFP to generate pLL5.0 or pLL5.0-EGFP-CPß respectively. Complimentary sequences were spliced using splice-overlap extension, followed by PCR to generate either 5'LTR-MCS-EGFP or 5'LTR-EGFP-CP. These sequences were cloned into pLL3.7 as NotI/MfeI fragments using standard techniques to replace the CMV-EGFP sequence (excised with NotI/EcoRI) from pLL3.7. Knock-down sequences were designed and cloned

as described previously [75] into either pLL3.7 or a red fluorescent protein version of pLL3.7, and sub-cloned into other pLL-based vectors as indicated, using standard techniques. Coro1B and SSH1L were cloned into the MCS of pLL5.0 using standard techniques. EGFP-actin was cloned as an EcoRI/ClaI(blunt) fragment into an EcoRI/SbfI(blunt) digested pLL5.0, replacing the EGFP. The bi-cistronic lenti-lox vector, pLL-5.5, was generated by replacing the GFP in pLL-5.0 (described in [80]) with the internal ribosomal entry sequence (IRES) from pQC-XIX using standard PCR-based cloning techniques.

Cell Culture, lentiviral infections and generation of clonal derivatives

HEK-293FT and Rat2 cells were cultured as described previously [81]. Lentiviral infections were carried out using standard protocols [75] and infected cell populations were FACS-sorted either for appropriate expression levels or to generate clonal derivatives, as indicated. Clonal CP-KDR cell lines were screened for appropriate expression by Western blot analysis using anti-CPß (3F2.3; 1:500) and anti-tubulin (E7; 1:1000) from Developmental Studies Hybridoma Bank, University of Iowa.

Immunofluoresence and Barbed-end Assays

Cells were plated on acid-washed coverslips coated with FN (100 µg/mL) and allowed to adhere overnight. Cells were fixed in ice-cold 4% paraformaldehyde for 10 minutes, and stained as previously described [18]. For barbed-end assays, cells were plated on FN-coated MatTek dishes and CALI was performed as described below. Without removing the dish from the microscope, cells were permeablized

with saponin buffer (20mM HEPES, 138 mM KCl, 4 mM MgCl2, 3 mM EDTA, 0.2 mg/mL saponin, 1% BSA, 1 mM ATP, 3 µm phalloidin) for 1 min, washed once in saponin-free buffer, and labeled for 3 min with 0.4 µM Alexa-568- conjugated G-actin (Molecular Probes). Cells were fixed with ice-cold 4% paraformaldehyde, washed with PBS and imaged immediately.

Live Cell Imaging, Tracking, Kymography and Actin Retrograde Flow

For live cell experiments, cells were adapted for several days to CO_2-independent imaging media: DME (Gibco) containing 4500 g/l glucose, 0.35 g/l $NaHCO_3$ and 25 mM HEPES, supplemented with 5% Fetal Bovine Serum (Hyclone), 100 units/ml penicillin, 100 mg/ml streptomycin and 292 mg/ml glutamine. Cells were plated on FN-coated delta-T imaging dishes (Bioptechs) and allowed to adhere prior to imaging. Migration of Rat2 fibroblasts was analyzed as described with slight modifications [18]. Cells were tracked and whole-cell speed calculated using Tracking Analysis software (Andor Bioimaging). GFP negative cells were analyzed as an internal control. For kymography, 300 images were captured at 1 s intervals and processed using ImageJ. Kymographs were generated from protrusive areas of at least 5 cells per treatment and lamellipodial parameters were calculated as described [82]. Data were exported to Prism for statistical analysis. For actin retrograde flow experiments, Rat2 cells infected pLL5.0-GFP-actin that contained either shCoro1B or shNS were used. Images were captured at 1 s intervals using spinning disk confocal microscopy. Kymographs were generated and analyzed as described above.

CALI protocol

EGFP-CP CALI experiments were performed by using a Spectra Physics Stabilite 2017 argon ion laser (Spectra Physics Laser Incorporated, 488 nm line, 2 W of beam power at the laser head) focused onto a 23.4 μm diameter spot ($1/e^2$ diameter) through a X60 1.45 N.A. PlanApo TIRF objective (Olympus). Irradiation was controlled with a fast Uniblitz shutter (Vincent Associates). Laser power at the specimen plane dropped to 625 mW because of optical losses and was measured by placing the sensor of a laser power meter (Model FM with LS 10 head, Coherent Inc.) directly above the objective. Irradiation time was 100 ms, resulting in a 62.5-mJ dose of energy for the CALI experiment.

CHAPTER 3: GOLGI POLARITY DOES NOT CORELATE WITH SPEED OR PERSISTENCE IN FREELY MIGRATING FIBROBLASTS

Summary

The polarization of the Golgi has long been thought to be important for cell migration. Here we show that Rat2 cells at the edge of an artificial wound repolarize the Golgi relative to the nucleus to face the direction of migration into the wound. However, in the absence of cues from neighboring cells, individual cells do not display Golgi polarity relative to the direction in which they are moving. Instead, the positioning of the Golgi relative to the nucleus remains relatively constant over time and does not reflect changes in the direction of migration. Consistent with this observation, we observe only a slight bias in Golgi positioning to the front of the nucleus and this bias is not higher during periods of time when the cell is moving in a persistent manner. Taken together, these data suggest that Golgi polarity is not a requirement for cell migration.

Introduction

Polarized cell migration is critical to many physiological processes including morphogenesis, immune response, and wound healing. One model for directional migration is the scratch-wound assay, in which a strip of cells are cleared from confluent monolayer and the remaining cells migrate collectively to fill the gap. In

this context, migration is accompanied by reorientation of the microtubule organizing center (MTOC), centrosome and Golgi apparatus, relative to the nucleus, to face the direction of migration (DOM). In general, manipulations that interfere with reorientation of the MTOC/centrosome or the Golgi also block migration into the wound [61, 63, 64]. It has therefore been assumed that centrosome/Golgi polarization is a fundamental step in cell migration, although this has not been tested directly.

Whether this holds true for cells outside the context of the wound edge is unclear. Few studies have addressed the importance of MTOC/centrosome polarity for the migration of single cells. In freely migrating PtK2 cells the centrosome did not reorient when the cell changed direction [74]. In *Dictyostelium*, the formation of a pseudopod precedes centrosome reorientation, and if this does not occur within 30 seconds, the pseudopod collapses [73]. These data suggest that centrosome positioning may be important for maintenance but not establishment of directed migration in freely migrating cells.

In this manuscript, we report for the first time the observation and analysis of Golgi position and morphology in live, freely migrating cells. Fluorescently tagged Golgi and nuclear markers were expressed in Rat2 fibroblasts and their positions were tracked in live cells. Contrary to the scratch-wound model, our data suggest that in freely migrating cells Golgi polarity is not a prerequisite for migration.

Results and Discussion

Polarity Sensor Validation

To assess whether Golgi polarity is related to migratory parameters, we developed a method to track the position of the Golgi apparatus relative to the nucleus in live cells over time. We designed a 'Polarity Sensor' to express fluorescent markers of both the nucleus (Histone H2B (H2B)-mCherry) and Golgi (ß-1,4-glactosyl transferase (GT)-EGFP) (Figure 4A). In Rat2 cells expressing this construct, GT-GFP co-localizes with the Golgi marker GM130 and H2B-mCherry co-localizes with Hoechst staining (Figure 4B). To confirm that Polarity Sensor expression did not affect polarization, we performed end-point scratch-wound assays and assessed Golgi polarity after 4 hours (Figure 4C, D). Cells were considered polarized if the centroid of the Golgi was within ±60° of the front of the nucleus (white lines, Figure 4C). We observed no significant difference in Golgi polarization between control cells and Polarity Sensor cells (77% vs. 71% respectively, $p > 0.05$, Figure 4D). Previous studies demonstrated that MTOC, and presumably Golgi polarity requires intact microtubules, and that low levels of nocodazole decreased MTOC reorientation [29, 61]. We observed a similar decrease in Golgi polarization in both cell lines when treated with low levels of nocodazole (50% vs. 51%, $p>0.05$, Figure 4D).

Heterogeneous Golgi Morphology in Sparsely Plated Cells

Polarity Sensor cells plated under low-density conditions for single-cell migration assays display a more heterogeneous morphology than cells in the

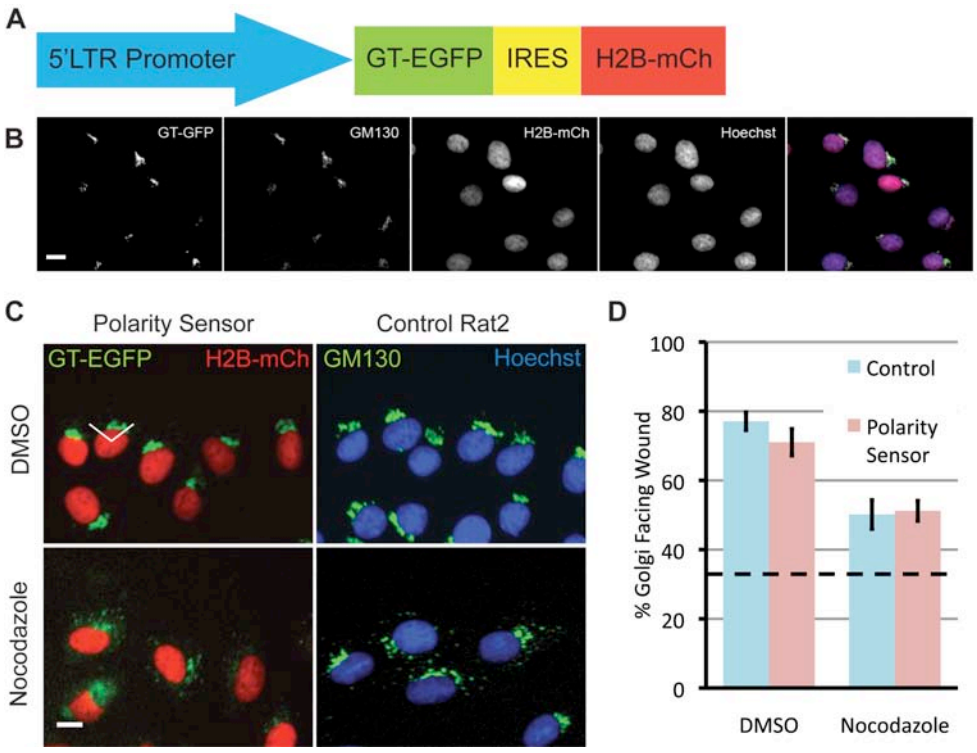

Figure 4: Characterization of the Polarity Sensor.

A) Polarity Sensor design. The Golgi is marked with the first 81 amino acids of ß-1,4-Glactosyl Transferase (GT) fused to EGFP. The nucleus is marked with histone H2B (H2B) fused to mCherry. These sequences flank an internal ribosomal entry sequence (IRES) to allow simultaneous expression from a single promoter.

B) Rat2 cells expressing the polarity sensor were fixed and stained with anti-GM130 and Hoechst. GT-GFP (green at right) and the Golgi marker GM130 (magenta) are co-localized, as are H2B-mCherry (red) and the nuclear stain, Hoechst (blue).

C) Representative images of cells in the scratch-wound assay treated with either DMSO (control) or nocodazole (0.1µg/mL). Uninfected Rat2 cells are labeled with anti-GM130 (green) and Hoëchst (blue) to mark the Golgi and nucleus, respectively. The wound edge is up, the white lines indicate ±60° facing the wound edge, considered polarized. Scale bar = 10 µm.

D) Quantification of results in (B). Results are from at least 100 cells per treatment from each of 3 independent experiments. Data were analyzed using one-way ANOVA and Turkey's post-test. Error bars = s.e.m.; dashed line indicates random Golgi positioning.

scratch-wound assay. We observed 7 categories of Golgi morphology (Figure 5A) and quantified the relative abundance of each type under different plating conditions (Figure 5B). For two categories, no clear Golgi centroid could be determined and these cells were excluded from analysis.

The Golgi Reorients to Face the Wound Edge in a Live-Cell Scratch-Wound Assay

Polarity Sensor cells were observed live in a scratch-wound assay using time-lapse microscopy (Figure 6A). Nuclear and Golgi positions were tracked by hand, as were cell positions because cell borders could not be unambiguously determined. From these three tracks, we calculated the Nuclear-Golgi Axis (NGA) and the current DOM at every time-point (Figure 6B). We plotted the angles of the current DOM and NGA vectors over time (Figure 6C). As expected, the NGA is initially random relative to the long-term DOM, but over time the Golgi becomes oriented to face into the wound. This trend was evident when we calculated the average absolute value of the NGA (|NGA|) for the population over time (Figure 6D). We also noticed that the current DOM fluctuated substantially despite the fact that this type of behavior was not evident in the time-lapse images. This likely reflects the fact that cells are moving slowly (<5 pixels per frame or <0.3 μm/min), and slight inaccuracies in tracking could result in significant fluctuations in the calculated current DOM (addressed below).

Freely Migrating Cells Have Rapid Changes in Direction Despite Constant Nucleus-Golgi Positioning

We next examined Golgi positioning in sparsely plated, freely migrating cells (Figure 6E). Cells underwent highly saltatory movement, characterized by periods of

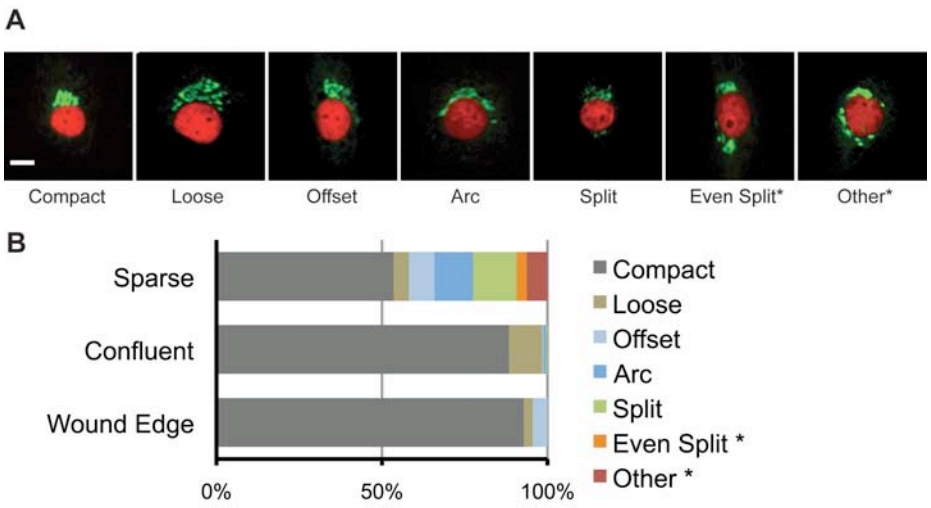

Figure 5: Golgi morphology is heterogeneous.

A) Representative images of different Golgi morphologies observed in sparsely plated cells. Scale bar = 10 µm.

B) Quantification of results in (A). Two categories of Golgi morphology, indicated by asterisks, were excluded from subsequent analyses because the Golgi position could not be determined.

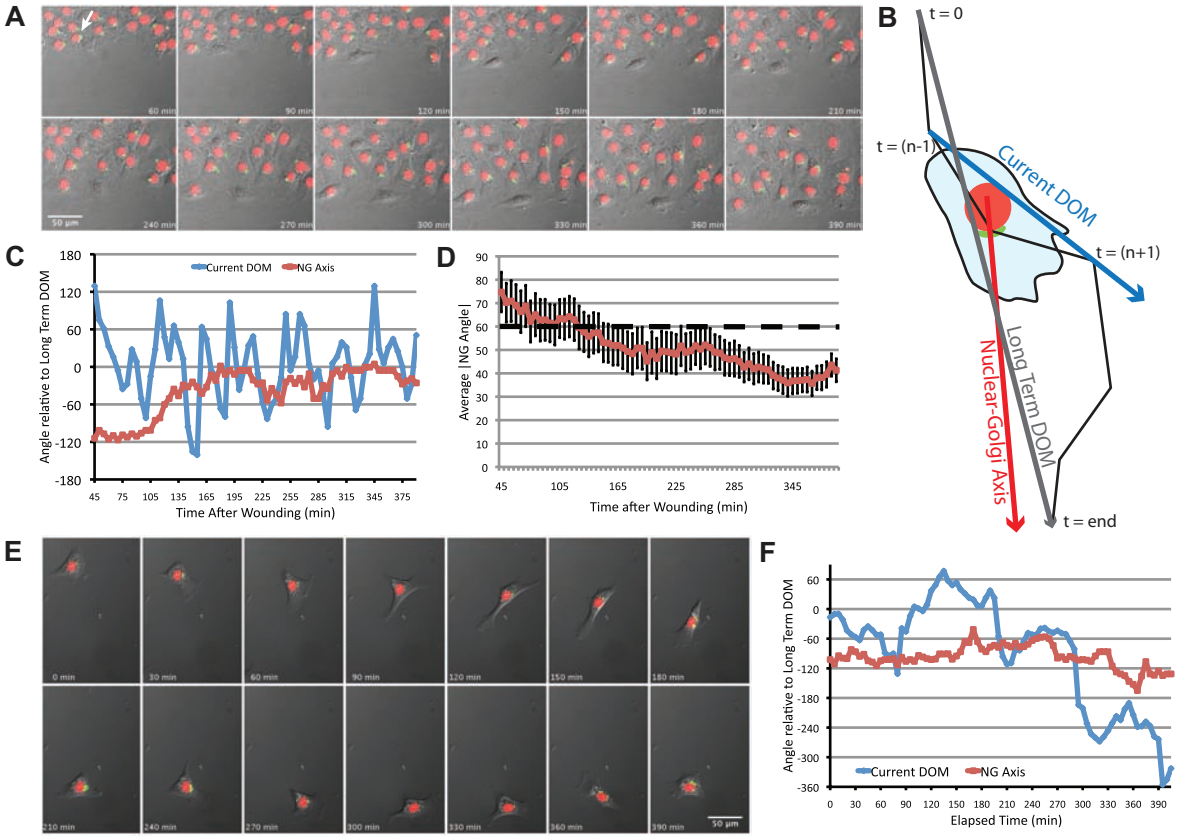

Figure 6: The Nuclear-Golgi Axis during migration.

A) Representative time-lapse images of Rat2 cells expressing the polarity sensor in the scratch-wound assay. The arrow indicates the cell analyzed in panel (C).

B) Schematic diagram of axes used for analysis. The cell track is represented by the black line, from t=0 to t=end. These two points define the long-term DOM (turquoise arrow). The current DOM at t=n is defined by the position of the cell centroid at t=(n-1) and t=(n+1) (blue arrow). The NGA is the vector defined by the current nuclear and Golgi positions (red arrow).

C) Current DOM and NGA relative to the long-term DOM over time for the representative cell indicated in panel (A).

D) The average absolute value of NGA relative to the long-term DOM for multiple cells (n~60) in the wound healing assay over time. Error bars = s.e.m.

E) Time-lapse images of a freely migrating cell expressing the polarity sensor.

F) Current DOM and NGA of cell in panel (E) relative to the long-term DOM over time. In this case, DOM was calculated from the hand-outlined track.

directionally persistent migration interspersed with periods of non-motility, or pauses, often associated with changes in direction. To minimize tracking inaccuracies revealed by our scratch-wound experiments (further investigated in Figure 7), we outlined cells in every frame and determined the mathematical centroid of the cell to generate more accurate cell tracks. We plotted the current DOM and the NGA over time (Figure 6F).

We were surprised to find that the NGA did not appear to align with either the current or long-term DOM. Rather Golgi positioning relative to the nucleus remains fairly constant over time, suggesting Golgi positioning is independent of the DOM in freely migrating cells. Changes in NGA are relatively slow, similar to a processing gyroscope. This 'gyroscope-like' behavior suggests that cells have the ability to maintain internal organization independent of peripheral structures such as the leading edge.

To investigate Golgi positioning during migration in a more quantitative way, we developed a metric (θ) of the relationship between the NGA and either the current DOM (θ_C) or the long term DOM (θ_{LT}) (Figure 8A). In either instance, a lower θ indicates that the NGA is more aligned with the specified DOM. For the scratch-wound assay, we used θ_{LT} since cells in this context were moving too slowly to accurately determine θ_C, but maintained constant direction for the duration of the assay. During wound closure, the Golgi was distributed within ±60° of the front of the nucleus 68.5% of the time (Figure 8B). This result is in general agreement with results from traditional end-point scratch-wound assays (Figure 4C).

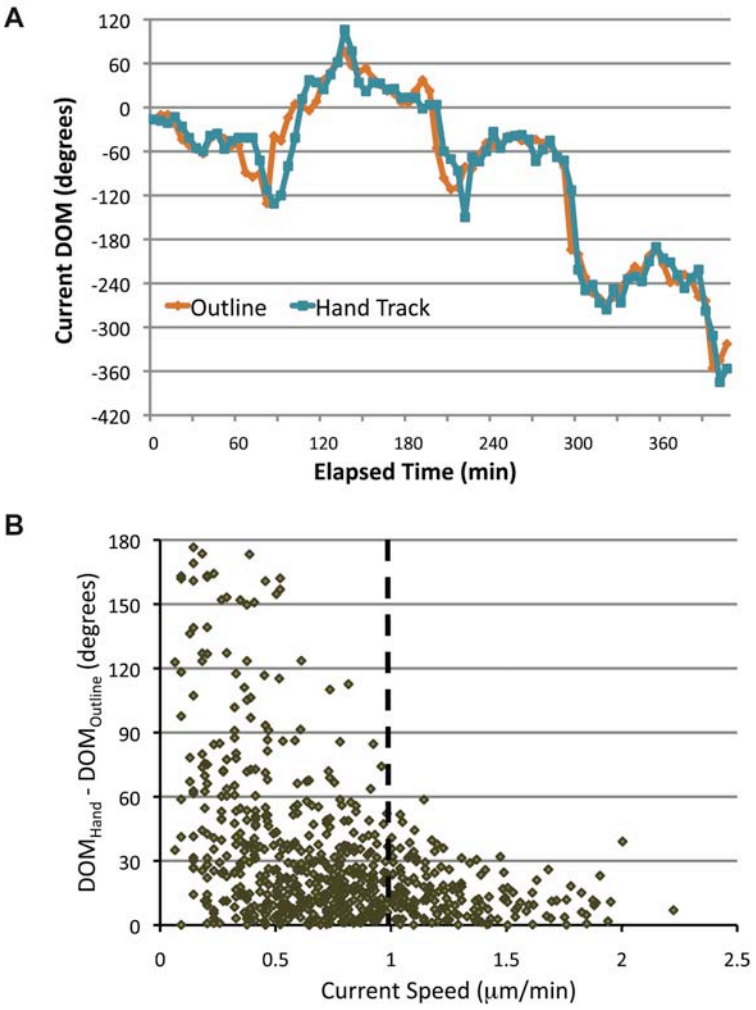

Figure 7: The direction of migration cannot be accurately determined by hand tracking when cells are moving slowly.

A) DOM was calculated from cell centroids determined by two different methods. Mathematical centroids were determined by outlining cells and using the measure function in ImageJ. Centroids of the same cells were also assessed by hand tracking. DOM was calculated for each tracking method and plotted over time for the cell in Fig. 2/3. There was general agreement in the current DOM between the two methods.

B) Difference in calculated DOM as a function of current cell speed. The DOM was determined for both data sets and the angle between these two directions was

plotted as a function of the distance traveled between two frames. At speeds below 1 μm/minute, hand tracking is unreliable for determining the direction of migration. Results are from 10 cells.

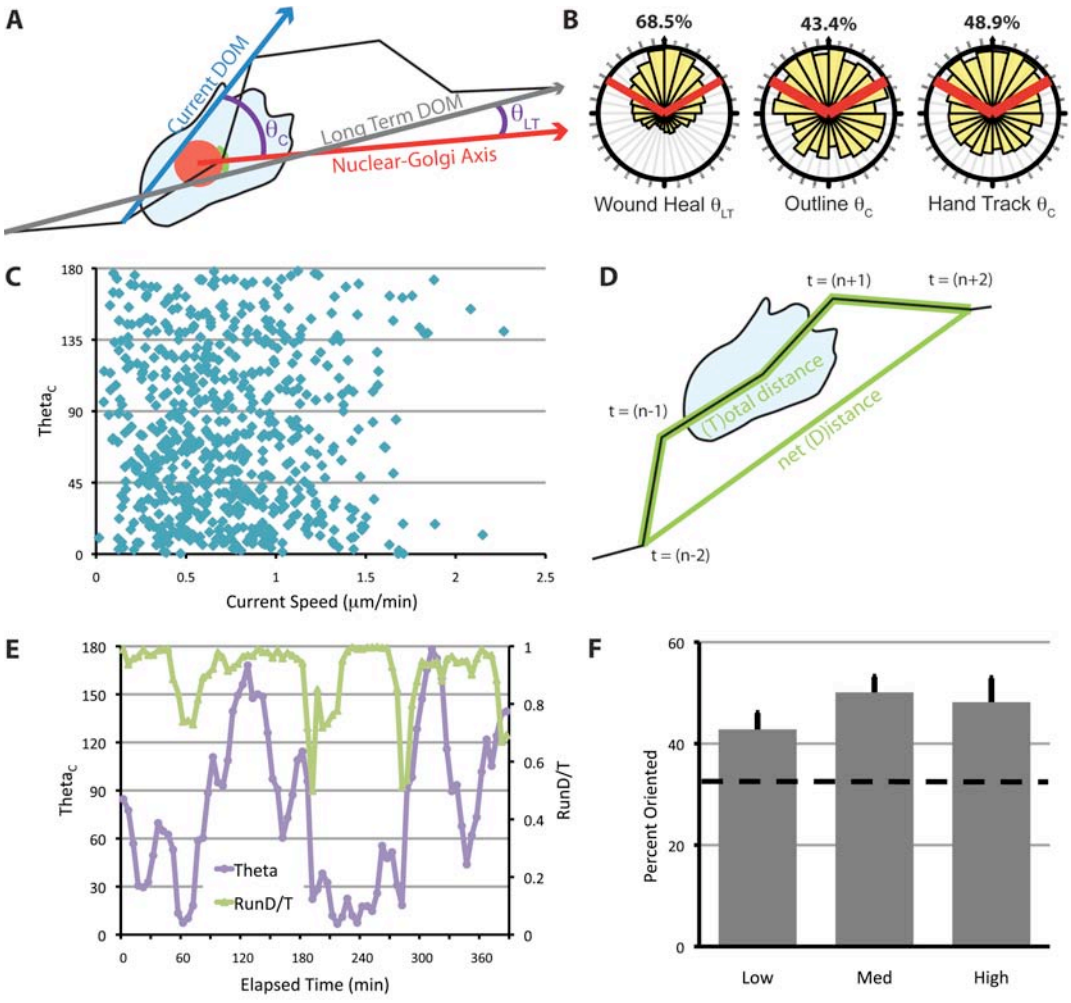

Figure 8: Nucleus-Golgi polarity is not correlated with the direction of migration in freely migrating cells.

A) Schematic for calculating θ. θ_{LT} is used for cells in the scratch wound assay and θ_C is used for freely migrating cells. The current DOM (and θ_C) was calculated from cell centroids determined in two ways, as described in the text and Fig. S1.

B) The distribution of θ for cells at the wound edge or in freely migrating cells. Red lines indicate ±60° facing the DOM, and the percentage of data that fall within these boundaries are indicated above. Data were generated from at least three independent experiments with at least 100 cells total for each condition, tracked over at least 5 hours.

C) **θ as a function of current cell speed. Current cell speed was calculated using tracks from outlined cells over 10 minutes from (t-1) to (t+1).**

D) **RunD/T was calculated as a sliding window using cell centroids from time (t-2), (t-1), (t), (t+1) and (t+2). D/T is defined as the net path length (D) divided by the total path length (T).**

E) **θ and RunD/T for the cell shown in Fig. 2E over time. RunD/T was calculated from the hand-outlined track of this cell.**

F) **Percentage of times when the Golgi is oriented (θ < 60°), during times when RunD/T is high (≥ 0.9), medium (0.9 > RunD/T > 0.7) or low (< 0.7) in freely migrating cells. RunD/T was calculated from the hand-tracked positions and instances when cells were deemed too slow for accurate tracking were eliminated (see Fig. S1). The dashed line indicates random Golgi positioning. Error bars = s.e.m. Data were generated from four independent experiments with at least 100 cells total.**

The frequent directional changes of freely migrating cells necessitated use of θ_C. Therefore, we calculated θ_C using either the accurate tracks from 10 outlined cells, or a larger cohort of hand tracked cells that were filtered to eliminate all instances when the cell was moving too slowly to track accurately (Figure 7B), and found that the Golgi was located in front of the nucleus approximately 45% of the time using either tracking method (Figure 8B). Together, these data indicate that freely migrating cells have less polarized Golgi than cells migrating into a wound.

Golgi Polarity is not Correlated With Cell Speed or Persistence

We examined the relationship between speed and θ_C for freely migrating cells (Figure 8C). In general, we see no correlation between cell speed and Golgi polarity. Since freely migrating fibroblasts are saltatory, we developed a new metric to monitor persistence over short periods by modifying a standard directionality measurement, D/T, which is normally calculated over the course of an entire experiment. Instead, we calculated D/T in a sliding window over 20 minutes, which we called RunD/T (Figure 8D). We examined the relationships between θ_C and RunD/T over the course of a typical experiment (Figure 8E) and observed no obvious relationship between these parameters (compare 120-180 min to 210-270 min, Figure 8E). To generalize this observation across multiple cells, we compared the fraction of time when a cell had an oriented Golgi (i.e. θC between ±60°) across three categories of RunD/T and found that Golgi polarization was equivalent (Figure 8F). This indicates that Golgi polarization is not correlated with speed or directional persistence in freely migrating cells.

Cells at the wound edge polarize the Golgi to face the direction of migration, yet freely migrating cells do not. Several factors present in the wound edge environment may account for this. First, cells at the wound edge can form junctional complexes with neighboring cells on all sides except the one facing into the wound. Recent evidence has demonstrated the importance of Cadherins in regulating MTOC/Golgi polarity at the wound edge [83-85]. Freely migrating cells lack junctional input, which results in an uncoupling of Golgi-nuclear positioning from peripheral events. Second, it has been shown that single cells will adopt specific orientation of the centrosome, Golgi and nucleus, without migrating, when plated on geometrically constrained substrates [86], suggesting that geometrical constrains can also impinge on Golgi polarity. The wound edge may provide the spatial and signaling cues that can drive MTOC/Golgi polarity - cues that are absent during single cell migration. The factor(s) responsible for determining the direction of migration in freely migrating cells have yet to be fully elucidated.

Materials and Methods

Materials

All materials were from Sigma unless otherwise indicated.

Generation of Polarity Sensor Cells

The polarity sensor vector was created in four basic steps. Primer sequences for all cloning steps are available on request. First, a bi-cistronic lenti-lox vector, pLL-5.5, was generated by replacing the GFP in pLL-5.0 (described in [80]) with the internal ribosomal entry sequence (IRES) from pQC-XIX using standard PCR-based

cloning techniques. Second, the Golgi-GFP marker was generated as follows. The sequence corresponding to the first 81 amino acids of human ß 1,4-galactosyltransferase (ß1,4-GT) was PCR-amplified from human first-strand DNA and cloned into pML2-EGFP(N1) as an EcoRI/BamHI fragment by standard techniques. The ß1,4-GT-GFP fragment was subcloned into pLL-5.5 as an EcoRI/NotI(blunt) fragment upstream of the IRES to generate pLL-5.5-GIX. Third, the nuclear-mCherry marker was generated as follows. Histone-H2B was amplified from mouse first strand DNA and cloned into pML2-mCherry(N1) as a SacII/SalI fragment. The Histone-H2B-mCherry fragment was PCR-amplified and cloned into the blunted pLL-5.5 vector downstream of the IRES to generate pLL-5.5-XIH. To create the final vector, pLL-5.5-GIH, we made use of the two internal PciI sites in pLL-5.5 (one in the IRES, another in the vector backbone) by ligating together two PciI fragments from pLL-5.5-GIX and pLL-5.5-XIH containing either ß1,4-GT-GFP or Histone-H2B-mCherry, respectively. Lentiviral infections of Rat2 fibroblasts were carried out as previously described [75, 82]. Individual Rat2 cells infected with pLL-5.5-GIH were cloned by fluorescence-activated cell-sorting and screened for appropriate levels of expression.

Cell Culture and Imaging Conditions

Cells (ATCC) were maintained as previously described [82]. For live cell experiments, cells were adapted for several days to CO_2-independent imaging media: DME (Gibco) containing 4500 g/l glucose, 0.35 g/l $NaHCO_3$ and 25 mM HEPES, supplemented with 5% Fetal Bovine Serum (Hyclone), 100 units/ml penicillin, 100 mg/ml streptomycin and 292 mg/ml glutamine. For live-cell scratch-

wound assays, cells were plated on laminin (LN)-coated (50 µg/ml) delta-T dishes (Bioptechs) at a density of 4.2x105 cells/dish. The following day, media was replaced with serum-free media containing 0.5% fatty acid-free BSA for 16-18hrs prior to assays. Confluent monolayers were wounded using a 200µl pipet tip, washed 2X with PBS and allowed to recover in imaging media containing 5% FBS for 45 minutes prior to imaging. For single-cell migration, cells were adapted and plated as above but at a density of 9.5x103 cells/dish and allowed to adhere overnight prior to imaging. For all live cell imaging, media was supplemented with 6-Hydroxy-2,5,7,8- tetramethylchroman-2-carboxylic acid (0.1mM), Ascorbate (0.5mM) and Catalase (10µg/ml).

End-Point Assays and Immunofluorescence

Cells were plated at the appropriate density on acid-washed LN-coated coverslips and allowed to adhere overnight. For nocodazole treatment, cells were pre-treated with 0.1µg/ml nocodazole for 1hr prior to wounding. Scratch assays were performed as above, and allowed to recover for 4 hours in serum-containing media (+/- nocodazole) prior to fixation. Cells were fixed as described [80] and stained with Hoechst (1:10 000, Invitrogen) and anti-GM130 (1:500, BD Transduction Laboratories) using standard techniques.

Image Acquisition and Analysis

Images were captured in Slidebook (Olympus) using an IX-81 Olympus inverted microscope with a 20X 0.75NA dry objective, a CCD camera (C4742-80-12AG, Hamamatsu) and an automated X-Y stage. Images were exported as tiff files

and analyzed using ImageJ. X-Y coordinates were exported to Excel (Microsoft) for calculations and graphing. Rose plots were generated in Aabel (Gigawiz, Ltd.) and statistical analysis was done in PRISM (Graph Pad, Inc.)

CHAPTER 4: GOLGI POSITIONING AND LAMELLIPODIAL DYNAMICS

Summary

Protrusion of the leading edge is an important factor in migration and requires delivery of signaling molecules. One possible source of the membrane and signaling complexes required for leading edge protrusion is the Golgi. We tested whether protrusion dynamics were related to the DOM or NGA. We find protrusion dynamics to be similar around the perimeter of the cell, regardless of Golgi positioning or DOM. This suggests that lamellipodial protrusion is not influenced by Golgi positioning and is not related to the DOM.

Introduction

Leading edge protrusion is thought to require the localized delivery of PM components, either through endosome recycling or through anterograde trafficking from the Golgi and trans-Golgi network (TGN) to the PM. In support of this, it was shown that Golgi-derived vesicles are transported farther from the Golgi and preferentially fuse close to the leading edge in cells at the wound edge compared with stationary confluent NRK fibroblasts [87]. Blocking TGN to PM transport by the expression of a kinase-dead protein kinase B (PKB) inhibits retrograde flow of surface particles, ruffling, and migration [88]. Lamellipodial dynamics in kinase-dead PKB expressing cells can be rescued by the expression of constitutively active Rac

[88], suggesting that Golgi-derived vesicles are not essential to provide bulk membrane for protrusion, however vesicle cargo could contain essential signaling complexes that might include Rac activators.

Combined with the observation that centrosome (and presumably Golgi) positioning is required for pseudopod stabilization in *Dictyostelium* one might speculate that the targeting of Golgi-derived vesicles to the leading edge provides signaling complexes that would help to establish or maintain “front-ness”. If this is the case, and post-Golgi vesicles do fuse preferentially to the front of the cell, we would expect to see protrusion dynamics affected by proximity to the Golgi. To determine whether this is true, we compared lamellipodial dynamics relative to the NGA and the DOM.

Results and Discussion

We examined lamellipodial dynamics in freely migrating Rat2 cells expressing the polarity sensor as described in Chapter 3. Lines for kymographs were drawn and classified as to whether they fell within ±30° of a specified axis (the long- or short-term DOM or the NGA, see Figure 9A). Lines that fell outside of these regions were used as a control. In general we saw minimal differences in the duration, distance, or rate of lamellipodial protrusions along the NGA relative to other regions (Figure 9B). There were two exceptions to this. First, the protrusion duration was moderately but significantly shorter along the NGA than in the control region. The significance of these results is unclear. If these data relect a true difference in protrusion duration, then Golgi positioning could serve to dampen lamellipodial dynamics. It is also possible that, although statistically significant, practically

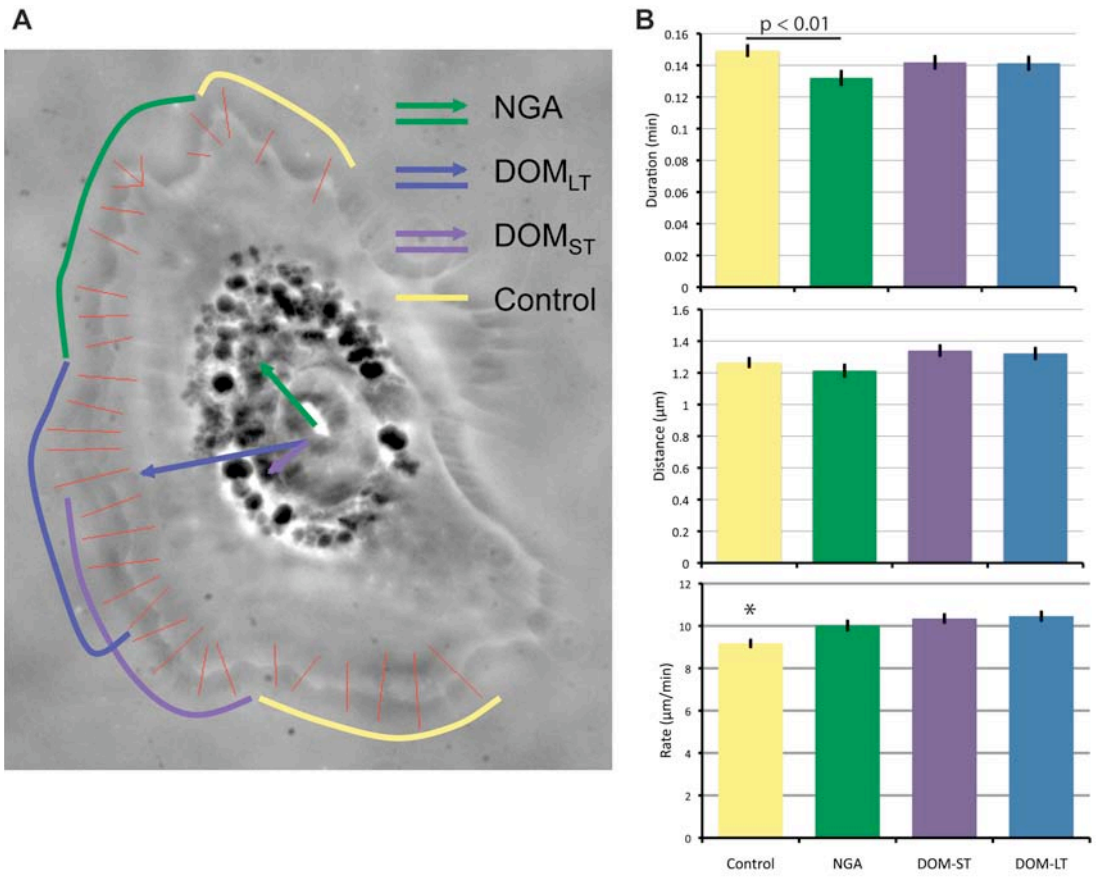

Figure 9: Lamellipodial dynamics relative to the NGA or DOM.

A) Representative image of a Rat2 cell expressing the polarity sensor with lines drawn for kymographs (red). Colored arrows represent the indicated axes, colored lines around the periphery indicate which kymograph lines fall within ±30° of the corresponding axis.

B) Quantification of the duration, distance and rates of protrusions along each axis. Data were generated from seven independent experiments with at least 18 cells total. The number of protrusion events analyzed for each category was at least 200. Data were analyzed using one-way ANOVA and Turkey's post-test. Except where indicated, all pair-wise comparisons were not significant ($p > 0.05$). Error bars = s.e.m. Asterisk indicates a significant difference ($p < 0.01$) from the other three regions.

speaking these differences are not substantial. In either case, Golgi positioning does not seem to increase lamellipodial dynamics.

The second significant result we obtained was that the protrusion rate was slightly but significantly slower in the control regions when compared with other regions. Again, it is not clear whether this represents a true difference in protrusion rate. If so, the extent to which this apparently negligible difference would contribute to net protrusive activity and migration should be investigated further. Regardless of whether differences in protrusion dynamics contribute to the DOM, a number of other factors that we have not accounted for could also influence the DOM. One possibility that we have not accounted for is the frequency of protrusion events, which could be higher in the DOM. Alternately, the dynamics or frequency of retraction events could be decreased in the DOM, leading to net protrusion. Finally, dynamics of contraction and retraction away from the leading edge (for example, retraction at the rear or the collapse of peripheral lamellipodia) could play a significant role in determining the DOM. Future studies could address these issues.

Materials and Methods

Materials and Cell Culture

All materials, cell lines and cell culture were as described in Chapter 3.

Imaging and Kymography

Red and green fluorescent images were taken at the beginning of imaging to determine nuclear and Golgi positions and calculate the NGA as described in Chapter 3. Movies for kymographs were generated by time-lapse imaging using

phase-contrast illumination at the rate of 1 image/second for 200 seconds. Cells were then imaged every 5 minutes for 25 minutes to determine the short-term (0-5 minutes) and long term (0-25 minutes) DOM. Maximum intensity projections were generated to aid in kymograph generation and analysis. Kymographs were classified as to whether they fell within 60° (±30°) of a specified axis (short- or long-term DOM, or NGA). Once kymographs were generated and classified, the distance, rate and persistence of protrusion were determined as described in Chapter 2. Data were exported to Excel (Microsoft) for graphical presentation and Prism (Graph Pad, Inc.) for statistical analysis.

CHAPTER 5: CONCLUSIONS AND FUTURE PROSPECTS

We have thus far described the development of a series of lentiviral-based expression constructs that enable the simultaneous knockdown of a target protein with the expression of either a rescue component, or a fluorescent marker to identify transduced cells. This system has allowed us to demonstrate not only the use of EGFP as a CALI chromophore, but also the necessity of eliminating endogenous labeled protein to observe the CALI effect. Furthermore, we have illustrated the utility of this system in analyzing the role of Coro1B in actin retrograde flow and SSH1L localization. Based on these results, current and ongoing studies in our lab utilizing this system, and the study on Golgi positioning discussed below, we anticipate its use for a broad range of applications in the future.

Using the bi-cistronic lenti-viral expression system to fluorescently tag the nucleus and Golgi, we have examined Golgi positioning relative to the nucleus in both freely migrating cells and cells migrating into an experimental wound. We found that in the context of the wound edge, the Golgi is reliably polarized to the front of the nucleus, as observed in other cell types [57, 59, 72, 89, 90]. In freely migrating cells however, the Golgi is much more randomly distributed, demonstrating that Golgi polarization is not a requirement for cell migration in this context. Furthermore, there does not seem to be a relationship between Golgi positioning and lamellipodial protrusion dynamics. Unfortunately, these results preclude the

possibility of testing the role(s) of various factors in polarity during random migration. On the other hand, these results do raise several interesting and more general issues with regard to Golgi positioning and morphology during random cell migration.

One issue worth considering is the morphology of the Golgi apparatus in different contexts. Although we observed a much more compact and homogeneous Golgi in confluent cells and those at the wound edge than in sparsely plated cells, the significance of this is unclear. Danson et al. found that RNAi against the actin regulator WAVE2 inhibited Golgi polarization at the wound edge and noted that the failure to polarize was accompanied by a 'fragmented Golgi' that resembled the Golgi of cells distant from the wound edge [89]. The authors suggest that this fragmentation and failure to polarize could be caused by disruption of the polarization signal to the Golgi. Although we do not see differences in Golgi morphology in Rat2 cells distant from the wound edge, we do find similar heterogeneous Golgi morphologies in freely migrating cells. It is possible that the signaling cascade involved in generating a compact Golgi morphology is not activated in freely migrating cells. Whether this would occur as a result of cell-cell signaling or geometric constraints is unknown. To address this, cells could be plated on small adhesive islands to provide geometric constraints in the absence of cell-cell contact. It would also be interesting to examine specific regulators of Golgi morphology and to determine the effect of their activities on Golgi behavior during different types of migration, or perhaps even their effects on migration itself. Candidates include members of the class I and II ADP-ribosylation factor (Arf) family of proteins (Arf1, Arf2, Arf3, Arf4 and Arf5), members of the ARAP (Arf GAP, Rho

GAP, ankyrin repeat, pleckstrin homology) and ASAP (Arf GAP, Src homology, ankyrin repeat, pleckstrin homology) families of Arf regulators, and other regulators of actin dynamics at the Golgi such as N-WASP, spectrin and cortactin (reviewed in [91]), or various combinations of these. Of particular interest would be an Arf1/Arf4 double knock-down, as this combination was shown to cause Golgi dispersal in HeLa cells [92]. The effects of this treatment on cellular migration are unknown but warrant further investigation.

Another issue worth considering is the effect of Golgi positioning on lamellipodial dynamics. Although potential relationships between Golgi positioning and lamellipodial dynamics were only partially characterized, we find no obvious relationship between Golgi positioning or the DOM and protrusion dynamics such as rate, distance and duration. Clearly, for cell migration to occur, the net protrusive activity (i.e. the balance between protrusion and retraction) must be greater towards the DOM. The fact that our observations show minimal differences in protrusive activity suggests either that these small differences can account for migration, or that some other migratory parameters (protrusion frequency or retraction dynamics) are more important in determining the DOM. This warrants further investigation. Because it was shown that post-Golgi vesicles fuse preferentially to the front of wound-edge cells [87], it would be interesting to see if Golgi positioning affects this. This should also be examined in freely migrating cells to determine whether post-Golgi vesicles fuse preferentially in the DOM or relative to Golgi positioning. Another possibility is that endosome dynamics are different around the cell periphery and contribute to migration. For example, endocytosis has been shown to mediate focal

adhesion turnover at the cell rear (reviewed in [93]) while lamellipodial formation and ruffling and the activation of Rac also depend on endosomal proteins [94]. It would therefore be informative to track endosome dynamics in migrating cells using GFP-tagged Rab5 to determine whether endosome dynamics correlate with either focal adhesion turnover or lamellipodial dynamics and thus the direction of migration. Likewise it would also be interesting to block endocytosis (via knock-down of dynamin, or various combinations of Arfs) and examine the effects on different types of migration.

The greatest question arising from our studies is why Golgi polarity is so different between the scratch-wound assay and freely migrating cells. Many factors have been implicated in Golgi polarity during migration at the wound edge. Cdc42 and PAK are required to restrict protrusions to the front of the cell [66]. Intact MTs are required to maintain MTOC positioning and Golgi morphology (reviewed in [62]). Actin retrograde flow and contractility is required for nuclear positioning, particularly in rearward movement of the nucleus [63]. All of these factors should be functioning and contribute to Golgi polarity in freely migrating cells; however, this is not the case. What is it that sets freely migrating cells apart from cells at the wound edge? In cells at the wound edge, the protrusion and contractility that define the front and back of the cell tend to be both sustained and spatially continuous, whereas in freely migrating cells they tend to be transient and spatially discontinuous. It is important to keep in mind that the front and back of cells at the wound edge are defined by the wound edge itself; that is, in cells at the wound edge, polarity may be externally imposed.

One of the external factors that could contribute to polarity at the wound edge is the physical constraint imposed by neighboring cells. This constraint occurs on all sides except the one facing the wound. It was demonstrated that cells adopt a specific orientation and positioning of the centrosome, Golgi, and nucleus when plated on geometrically constrained 2-dimensional surfaces [86]. Under these conditions, the cells were unable to migrate yet the centrosome and Golgi were positioned at the centre of the cell and the nucleus was positioned away from the longest adhesive edge. Further support for the notion that physical constraints can drive polarity comes from two studies demonstrating that the topography of the extracellular environment can dictate Golgi polarity [95, 96]. These studies showed that cells plated on narrow stripes of adhesive material adopt a polarized morphology with the Golgi behind the nucleus. As cells at the wound edge could be spatially restricted in a similar manner, these observations suggest that the physical constraints at the rear of wound edge cells can contribute to Golgi polarity.

A second external factor present at the wound edge but absent from single cells is signaling input from cell-cell contacts or junctions. The cadherin family of junctional proteins are homotypic single-pass transmembrane proteins involved in the formation of adherens junctions and in mediating membrane associations between adjacent cells (reviewed in [97]). Loss of E-cadherin from NRK-52E epithelial cells causes random centrosome polarity in wound edge cells without affecting migration [84]. Similarly, loss of N-cadherin from myofibroblasts also causes random Golgi polarity at the wound edge, although loss of N-cadherin also impinges on wound-edge migration [83]. Regardless, cadherin-based signaling

input from neighboring cells seems to be important for wound edge polarity. As the cadherins are linked to the actin cytoskeleton via the catenins this role in polarity could be mediated by influencing actin dynamics at sites of contact. Interestingly, a recent study demonstrated that the nucleus and centrosome were drawn away from the cell centroid towards sites of cadherin signaling in an actin-dependent manner [85]. Junctions could also have a secondary role in migration and polarity at the wound edge; maintaining junctions could restrain the rapid and highly saltatory type of migration observed in freely migrating cells. We do observe that cells at the wound edge move significantly more slowly than individual cells (not shown). However, the removal of ECM proteins during the scratching process could account for this. One way to examine this is to compare the migration rates of freely migrating cells and those at the wound edge when plated on either LN or uncoated glass. If the slow migration rates observed at the wound edge are comparable to freely migrating cells plated on uncoated glass we would expect that the slow migration rate at the wound edge is due to the lack of ECM proteins required for adhesion. However, if freely migrating cells migrate at the same rate on untreated glass as they do on LN, the potential removal of ECM from the wound does not likely contribute to the slower speed observed in cells at the wound edge. In either case, cadherin-based junctions likely play a role in mediating the Golgi polarity seen in wound edge cells but presumably could not contribute to polarity in freely migrating cells.

One model for how cells at the wound edge become polarized is described as follows: cells experience asymmetric cell-cell contact, leading to asymmetrical

intracellular signaling events through physical constraints, cadherin-based signaling, or both. Because cell-cell contact is maintained during migration – the back and sides are defined by cell-cell contact for indefinite periods of time – asymmetries in signaling are both spatially and temporally continuous. The constant reinforcement of 'front' and 'back' could allow the events at the cell periphery to affect or become coupled to the internal organization of the cell.

In contrast, freely migrating cells establish transient asymmetries in intracellular signaling, resulting in localized areas of protrusion and adhesion. Signaling is not only discontinuous around the periphery of the cell, but is perhaps not sustained for sufficient periods to affect positioning of the nucleus, centrosome or Golgi. If this model is correct, we would expect to see that cells undergoing persistent chemotaxis in which front/back signaling is constantly reinforced would also couple peripheral events to internal organization.

We have performed preliminary experiments to address Golgi positioning during chemotaxis (see Appendix). Unfortunately we were able to achieve chemotaxis only once, and in this instance DIC image quality was so poor as to render cell tracking impossible. We therefore used nuclear positions to generate cell tracks and calculate D/T and θ. Chemotaxis was indeed observed, as 36/43 cells migrated towards the chemotactic source. Based on the observed cell paths and the fact that the D/T was only marginally increased relative to freely migrating cells (not shown), the cells in this experiment were likely undergoing biased random walk chemotaxis rather than persistent chemotaxis [69]. Using nuclear positioning to calculate the DOM and θ_C, we found that Golgi polarity was comparable to that

observed in freely migrating cells, with the Golgi positioned to the front of the nucleus 47% of the time. Additionally, we did not observe any bias in Golgi positioning towards the chemotactic source, with the Golgi positioned up-gradient from the nucleus only 44% of the time. Together this suggests that biased random walk chemotaxis does not induce Golgi polarity. However, we did observe that the Golgi polarization was moderately increased along the long-term DOM, with the Golgi positioned to the front of the nucleus 53% of the time. The significance of this is not immediately apparent. As the majority of cells are migrating towards the chemotactic source, we would also expect to see a bias in Golgi positioning relative to the gradient, which we do not. However, based on the cell tracks, even cells that do exhibit net migration towards the source often do not migrate parallel to the gradient, even over the long term. It is possible that chemotaxing cells become elongated along the long-term DOM, which in turn could bias Golgi positioning to either the front or rear of the nucleus based purely on cell geometry. It was shown previously that cells migrating on 1D substrates also became elongated, however in this context the Golgi was positioned preferentially to the rear of the nucleus [95]. The extent to which elongation occurs in chemotaxing cells, and how or whether this contributes to Golgi positioning is not clear and requires further investigation. Ongoing efforts aim to address this.

APPENDIX

Chemotaxis in a Gradient of Serum

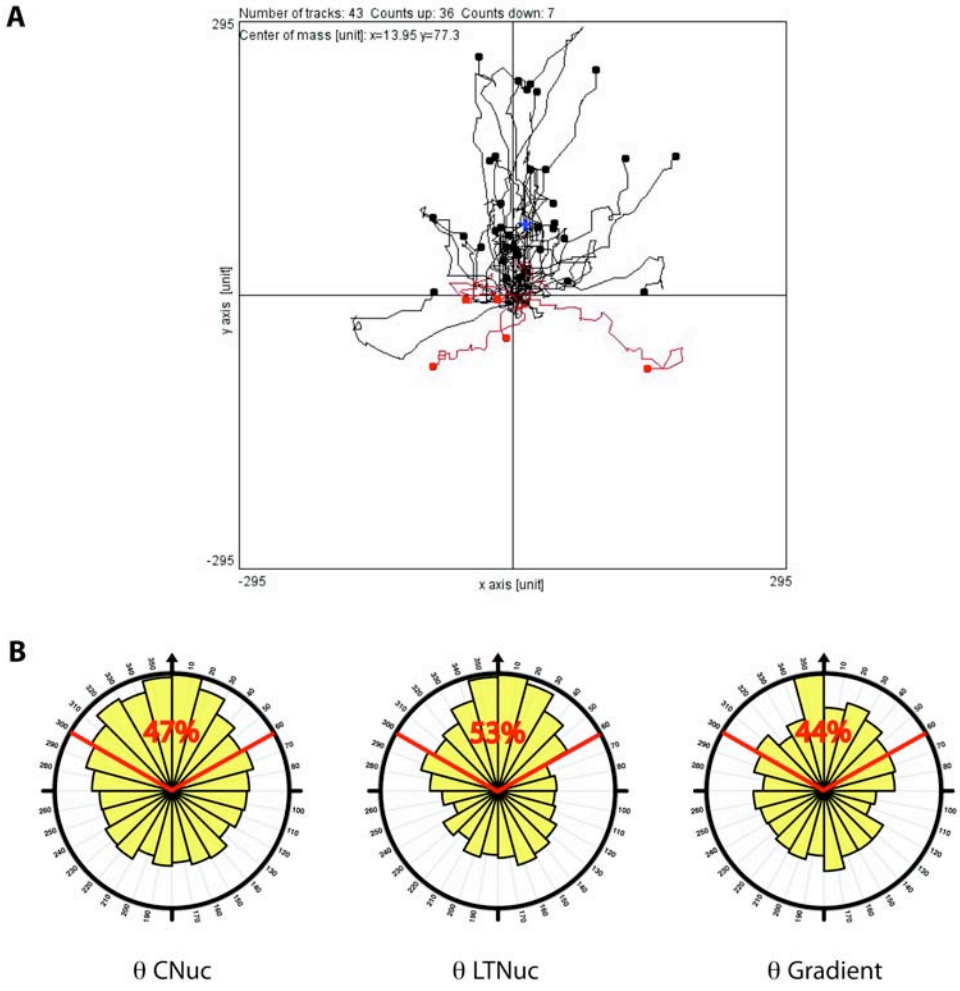

Figure 10: Chemotaxis in a gradient of serum.

A) Cell tracks of 43 cells migrating in the µ-slide chemotaxis chamber in a gradient of serum.

B) The distribution of θ for cells in the chemotaxis chamber. The current and long-term DOM was calculated using nuclear positions rather than cell positions. The gradient direction was used as a reference instead of the DOM for θ Gradient.

Materials and Methods

Cells were cultured as described in Chapter 3. Cells were plated on LN-coated (50 µg/ml, 37°C 1hr) ibidi µ-slide chemotaxis chambers (Integrated BioDiagnostics) as per the manufactures directions, and allowed to adhere for 2 hours in serum containing media. Media was then replaced and the chambers filled with serum free media and cells were serum starved for ~6 hours. Serum was introduced to the source chamber as per the manufacturers directions to a final concentration of 10% serum in the source chamber. Imaging was initiated 20 minutes after the introduction of serum as described in Chapter 3. Nucleus and Golgi positions were tracked essentially as described in Chapter 3. DIC image quality was poor, preventing tracking of cell positions. Theta was therefore calculated as described in Chapter 3 using nuclear positions in place of cell centroid positions.

REFERENCES

1. Ghashghaei H.T., Lai C., and Anton E.S. (2007). Neuronal migration in the adult brain: are we there yet? Nat Rev Neurosci. *8*, 141-151.
2. Christensen J.E., and Thomsen A.R. (2009). Co-ordinating innate and adaptive immunity to viral infection: mobility is the key. APMIS. *117*, 338-355.
3. Villablanca E.J., Russo V., and Mora J.R. (2008). Dendritic cell migration and lymphocyte homing imprinting. Histol Histopathol. *23*, 897-910.
4. Szekanecz Z., and Koch A.E. (2007). Macrophages and their products in rheumatoid arthritis. Curr Opin Rheumatol. *19*, 289-295.
5. Chiang A.C., and Massague J. (2008). Molecular basis of metastasis. N Engl J Med. *359*, 2814-2823.
6. Ridley A.J., Schwartz M.A., Burridge K., Firtel R.A., Ginsberg M.H., Borisy G., Parsons J.T., and Horwitz A.R. (2003). Cell migration: integrating signals from front to back. Science. *302*, 1704-1709.
7. van Rheenen J., Song X., van Roosmalen W., Cammer M., Chen X., Desmarais V., Yip S.C., Backer J.M., Eddy R.J., and Condeelis J.S. (2007). EGF-induced PIP2 hydrolysis releases and activates cofilin locally in carcinoma cells. J Cell Biol. *179*, 1247-1259.
8. Chung C.Y., and Firtel R.A. (2002). Signaling pathways at the leading edge of chemotaxing cells. J Muscle Res Cell Motil. *23*, 773-779.
9. Benard V., Bohl B.P., and Bokoch G.M. (1999). Characterization of rac and cdc42 activation in chemoattractant-stimulated human neutrophils using a novel assay for active GTPases. J Biol Chem. *274*, 13198-13204.
10. Akasaki T., Koga H., and Sumimoto H. (1999). Phosphoinositide 3-kinase-dependent and -independent activation of the small GTPase Rac2 in human neutrophils. J Biol Chem. *274*, 18055-18059.
11. Dise R.S., Frey M.R., Whitehead R.H., and Polk D.B. (2008). Epidermal growth factor stimulates Rac activation through Src and phosphatidylinositol 3-kinase to promote colonic epithelial cell migration. Am J Physiol Gastrointest Liver Physiol. *294*, G276-85.
12. Higgs H.N., and Pollard T.D. (2001). Regulation of actin filament network formation through ARP2/3 complex: activation by a diverse array of proteins. Annu Rev Biochem. *70*, 649-676.
13. Mullins R.D., Heuser J.A., and Pollard T.D. (1998). The interaction of Arp2/3 complex with actin: nucleation, high affinity pointed end capping, and formation of branching networks of filaments. Proc Natl Acad Sci U S A. *95*, 6181-6186.

14. Bailly M., Ichetovkin I., Grant W., Zebda N., Machesky L.M., Segall J.E., and Condeelis J. (2001). The F-actin side binding activity of the Arp2/3 complex is essential for actin nucleation and lamellipod extension. Curr Biol. *11*, 620-625.

15. Akin O., and Mullins R.D. (2008). Capping protein increases the rate of actin-based motility by promoting filament nucleation by the Arp2/3 complex. Cell. *133*, 841-851.

16. Mejillano M.R., Kojima S., Applewhite D.A., Gertler F.B., Svitkina T.M., and Borisy G.G. (2004). Lamellipodial versus filopodial mode of the actin nanomachinery: pivotal role of the filament barbed end. Cell. *118*, 363-373.

17. Goode B.L., and Eck M.J. (2007). Mechanism and function of formins in the control of actin assembly. Annu Rev Biochem. *76*, 593-627.

18. Cai L., Holoweckyj N., Schaller M.D., and Bear J.E. (2005). Phosphorylation of coronin 1B by protein kinase C regulates interaction with Arp2/3 and cell motility. J Biol Chem. *280*, 31913-31923.

19. Mseka T., Bamburg J.R., and Cramer L.P. (2007). ADF/cofilin family proteins control formation of oriented actin-filament bundles in the cell body to trigger fibroblast polarization. J Cell Sci. *120*, 4332-4344.

20. Vicente-Manzanares M., Koach M.A., Whitmore L., Lamers M.L., and Horwitz A.F. (2008). Segregation and activation of myosin IIB creates a rear in migrating cells. J Cell Biol. *183*, 543-554.

21. Wessels D., Lusche D.F., Kuhl S., Heid P., and Soll D.R. (2007). PTEN plays a role in the suppression of lateral pseudopod formation during Dictyostelium motility and chemotaxis. J Cell Sci. *120*, 2517-2531.

22. Xu J., Wang F., Van Keymeulen A., Herzmark P., Straight A., Kelly K., Takuwa Y., Sugimoto N., Mitchison T., and Bourne H.R. (2003). Divergent signals and cytoskeletal assemblies regulate self-organizing polarity in neutrophils. Cell. *114*, 201-214.

23. Servant G., Weiner O.D., Herzmark P., Balla T., Sedat J.W., and Bourne H.R. (2000). Polarization of chemoattractant receptor signaling during neutrophil chemotaxis. Science. *287*, 1037-1040.

24. Wang F., Herzmark P., Weiner O.D., Srinivasan S., Servant G., and Bourne H.R. (2002). Lipid products of PI(3)Ks maintain persistent cell polarity and directed motility in neutrophils. Nat Cell Biol. *4*, 513-518.

25. Weiner O.D., Neilsen P.O., Prestwich G.D., Kirschner M.W., Cantley L.C., and Bourne H.R. (2002). A PtdInsP(3)- and Rho GTPase-mediated positive feedback loop regulates neutrophil polarity. Nat Cell Biol. *4*, 509-513.

26. Srinivasan S., Wang F., Glavas S., Ott A., Hofmann F., Aktories K., Kalman D., and Bourne H.R. (2003). Rac and Cdc42 play distinct roles in regulating PI(3,4,5)P3 and polarity during neutrophil chemotaxis. J Cell Biol. *160*, 375-385.

27. Papakonstanti E.A., Ridley A.J., and Vanhaesebroeck B. (2007). The p110delta isoform of PI 3-kinase negatively controls RhoA and PTEN. EMBO J. *26*, 3050-3061.

28. Li Z., Dong X., Wang Z., Liu W., Deng N., Ding Y., Tang L., Hla T., Zeng R., Li L. et al. (2005). Regulation of PTEN by Rho small GTPases. Nat Cell Biol. *7*, 399-404.

29. Etienne-Manneville S., and Hall A. (2001). Integrin-mediated activation of Cdc42 controls cell polarity in migrating astrocytes through PKCzeta. Cell. *106*, 489-498.

30. Pankov R., Endo Y., Even-Ram S., Araki M., Clark K., Cukierman E., Matsumoto K., and Yamada K.M. (2005). A Rac switch regulates random versus directionally persistent cell migration. J Cell Biol. *170*, 793-802.

31. Li S., Guan J.L., and Chien S. (2005). Biochemistry and biomechanics of cell motility. Annu Rev Biomed Eng. *7*, 105-150.

32. Liu S., Calderwood D.A., and Ginsberg M.H. (2000). Integrin cytoplasmic domain-binding proteins. J Cell Sci. *113*, 3563-3571.

33. Zaidel-Bar R., Itzkovitz S., Ma'ayan A., Iyengar R., and Geiger B. (2007). Functional atlas of the integrin adhesome. Nat Cell Biol. *9*, 858-867.

34. Martel V., Racaud-Sultan C., Dupe S., Marie C., Paulhe F., Galmiche A., Block M.R., and Albiges-Rizo C. (2001). Conformation, localization, and integrin binding of talin depend on its interaction with phosphoinositides. J Biol Chem. *276*, 21217-21227.

35. Wegener K.L., Partridge A.W., Han J., Pickford A.R., Liddington R.C., Ginsberg M.H., and Campbell I.D. (2007). Structural basis of integrin activation by talin. Cell. *128*, 171-182.

36. Worth D.C., and Parsons M. (2008). Adhesion dynamics: mechanisms and measurements. Int J Biochem Cell Biol. *40*, 2397-2409.

37. Gingras A.R., Bate N., Goult B.T., Hazelwood L., Canestrelli I., Grossmann J.G., Liu H., Putz N.S., Roberts G.C., Volkmann N. et al. (2008). The structure of the C-terminal actin-binding domain of talin. EMBO J. *27*, 458-469.

38. Kaverina I., Krylyshkina O., and Small J.V. (2002). Regulation of substrate adhesion dynamics during cell motility. Int J Biochem Cell Biol. *34*, 746-761.

39. Alexandrova A.Y., Arnold K., Schaub S., Vasiliev J.M., Meister J.J., Bershadsky A.D., and Verkhovsky A.B. (2008). Comparative dynamics of retrograde actin flow and focal adhesions: formation of nascent adhesions triggers transition from fast to slow flow. PLoS One. *3*, e3234.

40. Bershadsky A.D., Ballestrem C., Carramusa L., Zilberman Y., Gilquin B., Khochbin S., Alexandrova A.Y., Verkhovsky A.B., Shemesh T., and Kozlov M.M. (2006). Assembly and mechanosensory function of focal adhesions: experiments and models. Eur J Cell Biol. *85*, 165-173.

41. Riveline D., Zamir E., Balaban N.Q., Schwarz U.S., Ishizaki T., Narumiya S., Kam Z., Geiger B., and Bershadsky A.D. (2001). Focal contacts as mechanosensors: externally applied local mechanical force induces growth of focal contacts by an mDia1-dependent and ROCK-independent mechanism. J Cell Biol. *153*, 1175-1186.

42. Kaverina I., Krylyshkina O., and Small J.V. (1999). Microtubule targeting of substrate contacts promotes their relaxation and dissociation. J Cell Biol. *146*, 1033-1044.

43. Glaven J.A., Whitehead I., Bagrodia S., Kay R., and Cerione R.A. (1999). The Dbl-related protein, Lfc, localizes to microtubules and mediates the activation of Rac signaling pathways in cells. J Biol Chem. *274*, 2279-2285.

44. Ren Y., Li R., Zheng Y., and Busch H. (1998). Cloning and characterization of GEF-H1, a microtubule-associated guanine nucleotide exchange factor for Rac and Rho GTPases. J Biol Chem. *273*, 34954-34960.

45. Kawasaki Y., Senda T., Ishidate T., Koyama R., Morishita T., Iwayama Y., Higuchi O., and Akiyama T. (2000). Asef, a link between the tumor suppressor APC and G-protein signaling. Science. *289*, 1194-1197.

46. Sanders L.C., Matsumura F., Bokoch G.M., and de Lanerolle P. (1999). Inhibition of myosin light chain kinase by p21-activated kinase. Science. *283*, 2083-2085.

47. Bershadsky A., Chausovsky A., Becker E., Lyubimova A., and Geiger B. (1996). Involvement of microtubules in the control of adhesion-dependent signal transduction. Curr Biol. *6*, 1279-1289.

48. Bhatt A., Kaverina I., Otey C., and Huttenlocher A. (2002). Regulation of focal complex composition and disassembly by the calcium-dependent protease calpain. J Cell Sci. *115*, 3415-3425.

49. Franco S.J., Rodgers M.A., Perrin B.J., Han J., Bennin D.A., Critchley D.R., and Huttenlocher A. (2004). Calpain-mediated proteolysis of talin regulates adhesion dynamics. Nat Cell Biol. *6*, 977-983.

50. Sampath R., Gallagher P.J., and Pavalko F.M. (1998). Cytoskeletal interactions with the leukocyte integrin beta2 cytoplasmic tail. Activation-dependent regulation of associations with talin and alpha-actinin. J Biol Chem. *273*, 33588-33594.

51. Gotlieb A.I., May L.M., Subrahmanyan L., and Kalnins V.I. (1981). Distribution of microtubule organizing centers in migrating sheets of endothelial cells. J Cell Biol. *91*, 589-594.

52. Caterina M.J., and Devreotes P.N. (1991). Molecular insights into eukaryotic chemotaxis. FASEB J. *5*, 3078-3085.

53. Firtel R.A., and Chung C.Y. (2000). The molecular genetics of chemotaxis: sensing and responding to chemoattractant gradients. Bioessays. *22*, 603-615.

54. Pu J., and Zhao M. (2005). Golgi polarization in a strong electric field. J Cell Sci. *118*, 1117-1128.

55. Lo C.M., Wang H.B., Dembo M., and Wang Y.L. (2000). Cell movement is guided by the rigidity of the substrate. Biophys J. *79*, 144-152.

56. Rhoads D.S., and Guan J.L. (2007). Analysis of directional cell migration on defined FN gradients: role of intracellular signaling molecules. Exp Cell Res. *313*, 3859-3867.

57. Kupfer A., Louvard D., and Singer S.J. (1982). Polarization of the Golgi apparatus and the microtubule-organizing center in cultured fibroblasts at the edge of an experimental wound. Proc Natl Acad Sci U S A. *79*, 2603-2607.

58. DeBiasio R., Bright G.R., Ernst L.A., Waggoner A.S., and Taylor D.L. (1987). Five-parameter fluorescence imaging: wound healing of living Swiss 3T3 cells. J Cell Biol. *105*, 1613-1622.

59. Yvon A.M., Walker J.W., Danowski B., Fagerstrom C., Khodjakov A., and Wadsworth P. (2002). Centrosome reorientation in wound-edge cells is cell type specific. Mol Biol Cell. *13*, 1871-1880.

60. Dow L.E., Kauffman J.S., Caddy J., Zarbalis K., Peterson A.S., Jane S.M., Russell S.M., and Humbert P.O. (2007). The tumour-suppressor Scribble dictates cell polarity during directed epithelial migration: regulation of Rho GTPase recruitment to the leading edge. Oncogene. *26*, 2272-2282.

61. Euteneuer U., and Schliwa M. (1992). Mechanism of centrosome positioning during the wound response in BSC-1 cells. J Cell Biol. *116*, 1157-1166.

62. Rios R.M., and Bornens M. (2003). The Golgi apparatus at the cell centre. Curr Opin Cell Biol. *15*, 60-66.

63. Gomes E.R., Jani S., and Gundersen G.G. (2005). Nuclear movement regulated by Cdc42, MRCK, myosin, and actin flow establishes MTOC polarization in migrating cells. Cell. *121*, 451-463.

64. Gotlieb A.I., Subrahmanyan L., and Kalnins V.I. (1983). Microtubule-organizing centers and cell migration: effect of inhibition of migration and microtubule disruption in endothelial cells. J Cell Biol. *96*, 1266-1272.

65. Etienne-Manneville S., and Hall A. (2003). Cdc42 regulates GSK-3beta and adenomatous polyposis coli to control cell polarity. Nature. *421*, 753-756.

66. Cau J., and Hall A. (2005). Cdc42 controls the polarity of the actin and microtubule cytoskeletons through two distinct signal transduction pathways. J Cell Sci. *118*, 2579-2587.

67. Hoeller O., and Kay R.R. (2007). Chemotaxis in the absence of PIP3 gradients. Curr Biol. *17*, 813-817.

68. Ferguson G.J., Milne L., Kulkarni S., Sasaki T., Walker S., Andrews S., Crabbe T., Finan P., Jones G., Jackson S. et al. (2007). PI(3)Kgamma has an important context-dependent role in neutrophil chemokinesis. Nat Cell Biol. *9*, 86-91.

69. Arrieumerlou C., and Meyer T. (2005). A local coupling model and compass parameter for eukaryotic chemotaxis. Dev Cell. *8*, 215-227.

70. Andrew N., and Insall R.H. (2007). Chemotaxis in shallow gradients is mediated independently of PtdIns 3-kinase by biased choices between random protrusions. Nat Cell Biol. *9*, 193-200.

71. Schliwa M., Pryzwansky K.B., and Euteneuer U. (1982). Centrosome splitting in neutrophils: an unusual phenomenon related to cell activation and motility. Cell. *31*, 705-717.

72. Nemere I., Kupfer A., and Singer S.J. (1985). Reorientation of the Golgi apparatus and the microtubule-organizing center inside macrophages subjected to a chemotactic gradient. Cell Motil. *5*, 17-29.

73. Ueda M., Graf R., MacWilliams H.K., Schliwa M., and Euteneuer U. (1997). Centrosome positioning and directionality of cell movements. Proc Natl Acad Sci U S A. *94*, 9674-9678.

74. Danowski B.A., Khodjakov A., and Wadsworth P. (2001). Centrosome behavior in motile HGF-treated PtK2 cells expressing GFP-gamma tubulin. Cell Motil Cytoskeleton. *50*, 59-68.

75. Rubinson D.A., Dillon C.P., Kwiatkowski A.V., Sievers C., Yang L., Kopinja J., Rooney D.L., Zhang M., Ihrig M.M., McManus M.T. et al. (2003). A lentivirus-based system to functionally silence genes in primary mammalian cells, stem cells and transgenic mice by RNA interference. Nat Genet. *33*, 401-406.

76. Marshall T.W., Aloor H.L., and Bear J.E. (2009). Coronin 2A regulates a subset of focal-adhesion-turnover events through the cofilin pathway. J Cell Sci. *122*, 3061-3069.

77. Guo J., Chen H., Puhl H.L.r., and Ikeda S.R. (2006). Fluorophore-assisted light inactivation produces both targeted and collateral effects on N-type calcium channel modulation in rat sympathetic neurons. J Physiol. *576*, 477-492.

78. Tour O., Meijer R.M., Zacharias D.A., Adams S.R., and Tsien R.Y. (2003). Genetically targeted chromophore-assisted light inactivation. Nat Biotechnol. *21*, 1505-1508.

79. Cai L., Makhov A.M., and Bear J.E. (2007). F-actin binding is essential for coronin 1B function in vivo. J Cell Sci. *120*, 1779-1790.

80. Cai L., Marshall T.W., Uetrecht A.C., Schafer D.A., and Bear J.E. (2007). Coronin 1B coordinates Arp2/3 complex and cofilin activities at the leading edge. Cell. *128*, 915-929.

81. Bear J.E., Loureiro J.J., Libova I., Fassler R., Wehland J., and Gertler F.B. (2000). Negative regulation of fibroblast motility by Ena/VASP proteins. Cell. *101*, 717-728.

82. Bear J.E., Svitkina T.M., Krause M., Schafer D.A., Loureiro J.J., Strasser G.A., Maly I.V., Chaga O.Y., Cooper J.A., Borisy G.G. et al. (2002). Antagonism between Ena/VASP proteins and actin filament capping regulates fibroblast motility. Cell. *109*, 509-521.

83. De Wever O., Westbroek W., Verloes A., Bloemen N., Bracke M., Gespach C., Bruyneel E., and Mareel M. (2004). Critical role of N-cadherin in myofibroblast invasion and migration in vitro stimulated by colon-cancer-cell-derived TGF-beta or wounding. J Cell Sci. *117*, 4691-4703.

84. Desai R.A., Gao L., Raghavan S., Liu W.F., and Chen C.S. (2009). Cell polarity triggered by cell-cell adhesion via E-cadherin. J Cell Sci. *122*, 905-911.

85. Dupin I., Camand E., and Etienne-Manneville S. (2009). Classical cadherins control nucleus and centrosome position and cell polarity. J Cell Biol. *185*, 779-786.

86. Thery M., Racine V., Piel M., Pepin A., Dimitrov A., Chen Y., Sibarita J.B., and Bornens M. (2006). Anisotropy of cell adhesive microenvironment governs cell internal organization and orientation of polarity. Proc Natl Acad Sci U S A. *103*, 19771-19776.

87. Schmoranzer J., Kreitzer G., and Simon S.M. (2003). Migrating fibroblasts perform polarized, microtubule-dependent exocytosis towards the leading edge. J Cell Sci. *116*, 4513-4519.

88. Prigozhina N.L., and Waterman-Storer C.M. (2004). Protein kinase D-mediated anterograde membrane trafficking is required for fibroblast motility. Curr Biol. *14*, 88-98.

89. Danson C.M., Pocha S.M., Bloomberg G.B., and Cory G.O. (2007). Phosphorylation of WAVE2 by MAP kinases regulates persistent cell migration and polarity. J Cell Sci. *120*, 4144-4154.

90. Magdalena J., Millard T.H., Etienne-Manneville S., Launay S., Warwick H.K., and Machesky L.M. (2003). Involvement of the Arp2/3 complex and Scar2 in Golgi polarity in scratch wound models. Mol Biol Cell. *14*, 670-684.

91. Myers K.R., and Casanova J.E. (2008). Regulation of actin cytoskeleton dynamics by Arf-family GTPases. Trends Cell Biol. *18*, 184-192.

92. Volpicelli-Daley L.A., Li Y., Zhang C.J., and Kahn R.A. (2005). Isoform-selective effects of the depletion of ADP-ribosylation factors 1-5 on membrane traffic. Mol Biol Cell. *16*, 4495-4508.

93. Tang B.L., and Ng E.L. (2009). Rabs and cancer cell motility. Cell Motil Cytoskeleton. *66*, 365-370.

94. Palamidessi A., Frittoli E., Garre M., Faretta M., Mione M., Testa I., Diaspro A., Lanzetti L., Scita G., and Di Fiore P.P. (2008). Endocytic trafficking of Rac is required for the spatial restriction of signaling in cell migration. Cell. *134*, 135-147.

95. Doyle A.D., Wang F.W., Matsumoto K., and Yamada K.M. (2009). One-dimensional topography underlies three-dimensional fibrillar cell migration. J Cell Biol. *184*, 481-490.

96. Pouthas F., Girard P., Lecaudey V., Ly T.B., Gilmour D., Boulin C., Pepperkok R., and Reynaud E.G. (2008). In migrating cells, the Golgi complex and the position of the centrosome depend on geometrical constraints of the substratum. J Cell Sci. *121*, 2406-2414.

97. Niessen C.M., and Gottardi C.J. (2008). Molecular components of the adherens junction. Biochim Biophys Acta. *1778*, 562-571.